

# Design, Preparation, and Characterization of Zn and Cu Metallopeptides Based On Tetradentate Aminopyridine Ligands Showing Enhanced DNA Cleavage Activity

Marta Soler,<sup>†,‡</sup> Eduard Figueras,<sup>‡</sup> Joan Serrano-Plana,<sup>†</sup> Marta González-Bártulos,<sup>§</sup> Anna Massaguer,<sup>§</sup> Anna Company,<sup>†</sup> M<sup>a</sup> Ángeles Martínez,<sup>§</sup> Jaroslav Malina,<sup>||</sup> Viktor Brabec,<sup>\*,||</sup> Lidia Feliu,<sup>\*,‡</sup> Marta Planas,<sup>\*,‡</sup> Xavi Ribas,<sup>\*,†</sup> and Miquel Costas<sup>\*,†</sup>

<sup>†</sup>QBIS-CAT Research Group, Institut de Química Computacional i Catàlisi (IQCC) and Departament de Química, Universitat de Girona, Campus Montilivi, E-17071 Girona, Catalonia, Spain

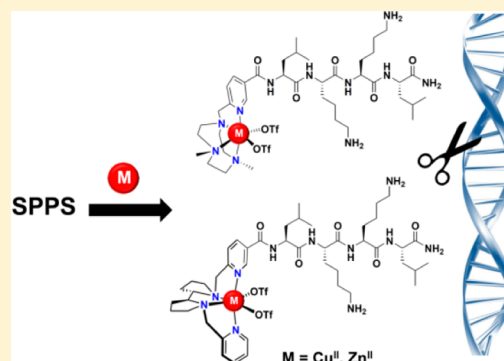
<sup>‡</sup>LIPPSO, Departament de Química, Universitat de Girona, Campus Montilivi, E-17071 Girona, Catalonia, Spain

<sup>§</sup>Biochemistry of Cancer Group, Biochemistry and Molecular Biology Unit, Department de Química and Department of Biology, Universitat de Girona, Campus Montilivi, 17071 Girona, Catalunya, Spain

<sup>||</sup>Institute of Biophysics, Academy of Sciences of the Czech Republic, v.v.i., Kralovopolska 135, CZ-61265 Brno, Czech Republic

## Supporting Information

**ABSTRACT:** The conjugation of redox-active complexes that can function as chemical nucleases to cationic tetrapeptides is pursued in this work in order to explore the expected synergistic effect between these two elements in DNA oxidative cleavage. Coordination complexes of biologically relevant first row metal ions, such as Zn(II) or Cu(II), containing the tetradentate ligands 1,4-dimethyl-7-(2-pyridylmethyl)-1,4,7-triazacyclononane (Me<sub>2</sub>PyTACN) and (2*S*,2*S'*)-1,1'-bis(pyrid-2-ylmethyl)-2,2'-bipyrrrolidine ((*S,S'*)-BPBP) have been linked to a cationic LKKL tetrapeptide sequence. Solid-phase synthesis of the peptide-tetradentate ligand conjugates has been developed, and the preparation and characterization of the corresponding metallotetrapeptides is described. The DNA cleavage activity of Cu and Zn metallopeptides has been evaluated and compared to their metal binding conjugates as well as to the parent complexes and ligands. Very interestingly, the oxidative Cu metallopeptides **1**<sub>Cu</sub> and **2**<sub>Cu</sub> show an enhanced activity compared to the parent complexes, [Cu(PyTACN)]<sup>2+</sup> and [Cu(BPBP)]<sup>2+</sup>, respectively. Under optimized conditions, **1**<sub>Cu</sub> displays an apparent pseudo first-order rate constant (*k*<sub>obs</sub>) of ~0.16 min<sup>-1</sup> with a supercoiled DNA half-life time (*t*<sub>1/2</sub>) of ~4.3 min. On the other hand, *k*<sub>obs</sub> for **2**<sub>Cu</sub> has been found to be ~0.11 min<sup>-1</sup> with *t*<sub>1/2</sub> ≈ 6.4 min. Hence, these results point out that the DNA cleavage activities promoted by the metallopeptides **1**<sub>Cu</sub> and **2**<sub>Cu</sub> render ~4-fold and ~23 rate accelerations in comparison with their parent Cu complexes. Additional binding assays and mechanistic studies demonstrate that the enhanced cleavage activities are explained by the presence of the cationic LKKL tetrapeptide sequence, which induces an improved binding affinity to the DNA, thus bringing the metal ion, which is responsible for cleavage, in close proximity.



## INTRODUCTION

Metallopeptides have emerged in recent years as versatile tools to explore new features in the bioinorganic discipline.<sup>1–5</sup> Particularly, redox-active metallopeptides are of potential use for different biological purposes, especially those involving DNA and RNA targeting.<sup>6–14</sup> For example, Barton and Cowan groups reported effective strategies in reaching DNA and RNA targets, therefore, constituting promising platforms for molecular probes and therapeutics.<sup>13,15</sup> Despite their interest, contributions of peptide-based transition metal complexes in this area are still relatively limited, usually hampered by their tedious synthetic preparation and characterization.<sup>16–18</sup> In this context, effective designs and straightforward synthetic methodologies must be addressed in order to obtain redox-active

metallopeptides that selectively interact with DNA.<sup>19–21,14,22</sup> Moreover, the same methodologies may provide inspiration for the further design of metallopeptide conjugates that can be endowed with cellular uptake properties for a nuclear-targeted accumulation.<sup>10,13,23,24</sup> This intracellular localization may undergo a redox-induced antiproliferative effect, similar to that mediated by the clinically approved iron chelated bleomycin.<sup>8</sup>

In this regard, peptides could be especially attractive templates to be considered as promising recognition sites in DNA-binding.<sup>12,25–30</sup> Particularly, the recognition specificity of

Received: April 22, 2015

positively charged short peptides toward DNA has been demonstrated. Facing the precedent literature, SPKK or KWKK cationic motifs have been reported to preferentially bind to the minor groove of the DNA with a degree of sequence specificity for A/T-rich sites.<sup>31–33</sup> This selective binding opens new perspectives for controlling the DNA interaction by molecules with useful properties.

On the basis of these precedents, in this work we have targeted the conjugation of cationic tetrapeptides to redox-active complexes that can function as chemical nucleases in order to explore the expected synergistic effect. As a model design, we focused our attention on the conjugation of complexes of biologically relevant first row metal ions, such as Zn(II) or Cu(II), containing the tetradentate ligands 1,4-dimethyl-7-(2-pyridylmethyl)-1,4,7-triazacyclononane (<sup>Me2</sup>PyTACN) and (2*S*,2*S'*)-1,1'-bis(pyrid-2-ylmethyl)-2,2'-bipyridine ((*S,S'*)-BPBP) to the cationic tetrapeptide LKKL. This sequence contains two consecutive lysine residues, which is analogous to the cationic motifs previously reported. Aminopyridine transition metal complexes with these ligands exhibit rich redox chemistry. Their high reactivity can be traced in the first place to the presence of labile sites in the metal ion coordination sphere that enable fast reaction with external molecules. For example, it has been shown that these sites enable fast reactivity of the iron and manganese complexes with peroxides, forming metal based reactive species.<sup>34–38</sup> Furthermore, metal complexes containing the former tetradentate ligands have been described as powerful and selective catalysts that operate under mild experimental conditions, and at the basis of this activity is the ability of these ligands to enable the metal ion to reach highly electrophilic high oxidation states.<sup>34–42</sup> This chemical behavior should be regarded as a significant difference from most common approaches in this topic that rely on chemically more stable complexes to form metalloproteins.

Aiming at taking advantage of the high reactivity of this class of complexes in a biological frame, herein, we report the solid-phase synthesis and the characterization of novel metal-tetrapeptides based on <sup>Me2</sup>PyTACN and (*S,S'*)-BPBP ligands. Furthermore, the DNA cleavage activity of Cu(II) and Zn(II) metalloproteins as a model for redox and hydrolytic DNA cleavage, respectively, have been studied and compared to their metal binding conjugates as well as to the parent complexes and ligands. Kinetic and binding assays as well as additional mechanistic studies have also been examined.

## EXPERIMENTAL SECTION

**Materials and Methods.** Unless otherwise stated, common chemicals and solvents (HPLC-grade or reagent-grade quality) were purchased from commercial sources and used without further purification. Solvents were dried by passing through an activated alumina purification system (MBraun SPS-800). The 9-fluorenylmethoxycarbonyl (Fmoc) derivatives and 4-methylbenzylhydramine (MBHA) resin (0.56 mmol/g) were obtained from Senn Chemicals International (Gentilly, France), NovaBiochem (Schwalbach, Germany), or IRIS Biotech GmbH (Marktredwitz, Germany). Amino-methyl ChemMatrix resin (0.66 mmol/g) was obtained from Matrix Innovation Inc. (St-Hubert, Canada). Ethyl 2-cyano-2-(hydroxyimino)acetate (Oxyma) and 1-[(1-(cyano-2-ethoxy-2-oxoethylideneaminoxy) dimethylaminomorpholino)] uronium hexafluorophosphate (COMU) were purchased from Novabiochem (Nottingham, UK). Trifluoroacetic acid (TFA), triisopropylsilane (TIS), dimethyl sulfoxide (DMSO), *N,N'*-diisopropylcarbodiimide (DIPC-DI), *N,N'*-diisopropylethylamine (DIPEA), picolinaldehyde, 4-

(dimethylamino)pyridine (DMAP), (*S,S*)-bypirrolidine, dimethylpyridine-2,5-dicarboxylate, *tert*-butyldimethylsilyl chloride (TBSCL), imidazole, 4-(dimethylamino)pyridine (DMAP), CaCl<sub>2</sub>, LiOH, NaBH<sub>4</sub>, (+)-sodium L-ascorbate, ethylenediaminetetraacetic acid (EDTA), 4,5-dihydroxy-1,3-benzenedisulfonic acid (Tiron), sodium azide, methyl green zinc chloride, and Hoechst were from Sigma–Aldrich Corporation (Madrid, Spain). Piperidine, tetrabutylammonium fluoride (TBAF), and *p*-toluenesulfonyl chloride (TsCl) were purchased from Fluka (Buchs, Switzerland). Anhydrous MgSO<sub>4</sub>, NaI, and acetic acid (AcOH) were purchased from Panreac (Barcelona, Spain). Aqueous NH<sub>3</sub> was obtained from Merck Millipore (USA). *N*-Methyl-2-pyrrolidinone (NMP), *N,N*-dimethylformamide (DMF), CH<sub>3</sub>OH, CH<sub>2</sub>Cl<sub>2</sub>, CH<sub>3</sub>CN, hexane, diethyl ether, and solvents for high performance liquid chromatography (HPLC) were obtained from Scharlau (Sentmenat, Spain). AcOEt and tetrahydrofuran (THF) were obtained from Carlo Erba (Milan, Italy). The pUC18 DNA was purchased from Thermo Fisher Scientific (Waltham, MA, USA).

Compounds were analyzed under standard analytical HPLC conditions with a Dionex liquid chromatography instrument composed of an UV/vis Dionex UVD170U detector, a P680 Dionex bomb, an ASI-100 Dionex automatic injector, and CHROMELEON 6.60 software. Detection was performed at 220 nm. Solvent A was 0.1% aq. TFA and solvent B was 0.1% TFA in CH<sub>3</sub>CN. Method A: Analysis was carried out with a Kromasil 100 C<sub>18</sub> (4.6 mm × 40 mm, 3.5 μm) column with a 2–100% B linear gradient over 7 min at a flow rate of 1 mL/min. Method B: Analysis was carried out with a Kromasil 100 C<sub>18</sub> (4.6 mm × 250 mm, 5 μm) column with a 2–100% B linear gradient over 30 min at a flow rate of 1 mL/min.

Reverse-phase column chromatography was carried out on a Teledyne ISCO CombiFlash RF-200 automated flash chromatography system using a RediSep Rf Gold reverse-phase C<sub>18</sub> column packed with high performance C<sub>18</sub> derivatized silica (Vertex Technics).

Analytical thin layer chromatography (TLC) was performed on precoated TLC plates, silica gel 60 F<sub>254</sub> (Merck). The spots on the TLC plates were visualized with UV/vis light (254 nm) and/or stained with a solution of potassium permanganate (1.5 g/100 mL H<sub>2</sub>O). Flash chromatography purifications and basifications were performed on silica gel 60 (230–400 mesh, Merck).

Electrospray ionization mass spectrometry (ESI-MS) analyses were performed with an Esquire 6000 ESI ion Trap LC/MS (Bruker Daltonics) instrument equipped with an electrospray ion source (University of Girona). The instrument was operated in the positive ESI(+) ion mode. Samples (5 μL) were introduced into the mass spectrometer ion source directly through an HPLC autosampler. The mobile phase (80:20 CH<sub>3</sub>CN/H<sub>2</sub>O at a flow rate of 100 μL/min) was delivered by a 1100 Series HPLC pump (Agilent). Nitrogen was employed as both the drying and nebulizing gas. High-resolution mass spectra (HRMS) were recorded under conditions of ESI with a Bruker MicrOTOF-Q IITM instrument using a hybrid quadrupole time-of-flight mass spectrometer (University of Girona). Samples were introduced into the mass spectrometer ion source by direct infusion through a syringe pump and were externally calibrated using sodium formate. The instrument was operated in the positive ESI(+) ion mode.

UV/vis spectroscopy was performed on an Agilent 8452 UV/vis spectrophotometer with 1 cm quartz cell, equipped with a temperature control cryostat from Unisoku Scientific Instruments, Japan.

<sup>1</sup>H and <sup>13</sup>C NMR spectra were measured with a Bruker 400 MHz NMR spectrometer (University of Girona). Chemical shifts were reported as δ values (ppm) directly referenced to the solvent signal.

Microwave-assisted reactions were performed with a single mode Discover S-Class labstation microwave (CEM) (0–300 W). The time, temperature, and power were controlled with the Synergy software. The temperature was monitored through an infrared sensor in the floor of the cavity.

Ethidium bromide (EB) was purchased from Merck KGaA. Calf thymus (ct) DNA, poly(dG-dC)<sub>2</sub>, and poly(dA-dT)<sub>2</sub> were purchased from Sigma (Prague, Czech Republic) and were used without further purification. The polynucleotides and ct-DNA were dissolved in 10

mM NaCl and kept frozen until the day of the experiment. The DNA concentrations (moles of bases per liter) of all polynucleotides were determined spectroscopically by using the published molar extinction coefficients at the maximum of the long wavelength absorbance.

**Synthesis.** *Synthesis of Methyl 6-(hydroxymethyl)nicotinate (9).* This compound was prepared following a slightly modified procedure with respect to the previously reported one.<sup>43</sup> A solution of dimethylpyridine-2,5-dicarboxylate (5 g, 0.025 mol) and CaCl<sub>2</sub> (11.35 g, 0.1 mol) in THF/CH<sub>3</sub>OH (1:2, 160 mL) was cooled to 0 °C, and NaBH<sub>4</sub> (1.45 g, 0.037 mol) was added slowly. The reaction was maintained at 0 °C and monitored by TLC. After consumption of the starting material, H<sub>2</sub>O (100 mL) was added slowly. The product was extracted with CHCl<sub>3</sub> (6 × 40 mL), and the combined organic layers were dried with anhydrous MgSO<sub>4</sub>. The solvent was evaporated under reduced pressure yielding an off white solid, which was purified by column chromatography. Elution with hexane/AcOEt (1:1) afforded methyl 6-(hydroxymethyl)nicotinate (**9**) as a white solid (4 g, 80% yield). *R*<sub>F</sub>: 0.82 hexane/AcOEt (1:7). <sup>1</sup>H NMR (400 MHz, CDCl<sub>3</sub>): δ = 3.95 (s, 3 H, OCH<sub>3</sub>), 4.83 (s, 2 H, CH<sub>2</sub>OH), 7.36 (dd, *J* = 0.6 and 8.2 Hz, 1 H, H<sub>5</sub>), 8.29 (dd, *J* = 2.0 and 8.2 Hz, 1 H, H<sub>4</sub>), 9.15 (dd, *J* = 0.6 and 2.0 Hz, 1 H, H<sub>2</sub>) ppm. <sup>13</sup>C NMR (100 MHz, CDCl<sub>3</sub>): δ = 52.4 (CH<sub>3</sub>O), 64.3 (CH<sub>2</sub>OH), 120.0 (C<sub>5</sub>), 124.9 (C<sub>3</sub>), 137.8 (C<sub>4</sub>), 149.9 (C<sub>2</sub>), 163.5 (C<sub>6</sub>), 165.6 (C=O) ppm. MS (ESI): *m/z* = 168.0 [M + H]<sup>+</sup>.

*Synthesis of Methyl 6-[(tert-butyl)dimethylsilyloxy]methyl]nicotinate.* Methyl 6-(hydroxymethyl)nicotinate (**9**) (2 g, 0.012 mol), imidazole (2.44 g, 0.036 mol), and DMAP (20 mg, 0.163 mmol) were dissolved in anhydrous CH<sub>3</sub>CN (60 mL) and stirred for 10 min at room temperature under nitrogen. After this time, TBSCl was added, and the reaction mixture was maintained for 2 h at room temperature under nitrogen. The reaction was monitored by TLC and, after the consumption of the starting material, H<sub>2</sub>O (50 mL) was added. The product was extracted with AcOEt (5 × 60 mL) and the combined organic layers were dried with anhydrous MgSO<sub>4</sub>. The solvent was evaporated under reduced pressure yielding methyl 6-[(tert-butyl)dimethylsilyloxy]methyl]nicotinate as a viscous yellow oil (1.72 g, 86% yield). *R*<sub>F</sub>: 0.68 (AcOEt/CH<sub>3</sub>OH/NH<sub>3</sub>(aq), 5:1:1). <sup>1</sup>H NMR (400 MHz, CDCl<sub>3</sub>): δ = 0.13 (s, 6 H, (CH<sub>3</sub>)<sub>2</sub>Si), 0.96 (s, 9 H, (CH<sub>3</sub>)<sub>3</sub>), 3.95 (s, 3 H, OCH<sub>3</sub>), 4.88 (s, 2 H, CH<sub>2</sub>O), 7.61 (dd, *J* = 0.4 and 8.0 Hz, 1 H, H<sub>5</sub>), 8.31 (dd, *J* = 2.0 and 8.0 Hz, 1 H, H<sub>4</sub>), 9.10 (dd, *J* = 0.4 and 2.0 Hz, 1 H, H<sub>2</sub>) ppm. <sup>13</sup>C NMR (100 MHz, CDCl<sub>3</sub>): δ = -5.3 (CH<sub>3</sub>)<sub>2</sub>Si, 18.5 (C(CH<sub>3</sub>)<sub>3</sub>), 26.0 ((CH<sub>3</sub>)<sub>3</sub>), 52.5 (CH<sub>3</sub>O), 66.1 (CH<sub>2</sub>), 119.6 (C<sub>5</sub>), 124.4 (C<sub>3</sub>), 138.0 (C<sub>4</sub>), 150.1 (C<sub>2</sub>), 166.0 (C<sub>6</sub>), 166.2 (C=O) ppm. MS (ESI): *m/z* = 282.1 [M + H]<sup>+</sup>.

*Synthesis of 6-[(tert-Butyl)dimethylsilyloxy]methyl]nicotinic acid (5).* This compound was prepared following a slightly modified procedure with respect to the previously reported.<sup>44</sup> An aqueous solution of LiOH (1.6 M, 10.65 mmol) was added dropwise to a solution of methyl 6-[(tert-butyl)dimethylsilyloxy]methyl]nicotinate (1 g, 3.55 mmol) in THF/CH<sub>3</sub>OH (1:1, 13.5 mL) at 0 °C. The reaction mixture was stirred at 0 °C for 30 min and at room temperature for 1.5 h. After this time, the solvent was evaporated under reduced pressure. Final pH adjustment was not performed to avoid the premature removal of the TBS group. Compound **5** was obtained as a white solid (0.75 g, 75% yield). This compound must be readily used because it was observed a partial TBS group removal after a few days of preparation. *R*<sub>F</sub>: 0.12 AcOEt/CH<sub>3</sub>OH/NH<sub>3</sub>(aq) (5:1:1). <sup>1</sup>H NMR (400 MHz, [D<sub>6</sub>]DMSO): δ = 1.66 (s, 15 H, (CH<sub>3</sub>)<sub>2</sub>Si, (CH<sub>3</sub>)<sub>3</sub>), 4.55 (s, 2 H, CH<sub>2</sub>O), 7.37 (dd, *J* = 1.0 and 10.8 Hz, 1 H, H<sub>5</sub>), 8.14 (dd, *J* = 2.8 and 10.8 Hz, 1 H, H<sub>4</sub>), 8.89 (dd, *J* = 1.0 and 2.8 Hz, 1 H, H<sub>2</sub>) ppm. MS (ESI): *m/z* = 266.1 [M - H]<sup>-</sup>.

*Synthesis of Methyl 6-(chloromethyl)nicotinate.* Methyl 6-(hydroxymethyl)nicotinate (**9**) (200 mg, 1.19 mmol) was dissolved in CH<sub>2</sub>Cl<sub>2</sub> (3.5 mL). SOCl<sub>2</sub> (200 μL, 2.75 mmol) was cautiously added dropwise, and the mixture was stirred overnight at room temperature. The solvent was removed by bubbling nitrogen into the crude reaction mixture (gaseous HCl is formed during this process and extreme caution must be taken) and a greenish solid was obtained. This product was suspended in Et<sub>2</sub>O (3.5 mL) and stirred for 1 h to give a fine solid which was then filtered, washed with Et<sub>2</sub>O (2 × 5 mL),

and dried under vacuum. Methyl 6-(chloromethyl)nicotinate was obtained as a white solid (188 mg, 85%). *R*<sub>F</sub>: 0.62 (AcOEt/CH<sub>3</sub>OH/NH<sub>3</sub>(aq), 5:1:1). <sup>1</sup>H NMR (400 MHz, CDCl<sub>3</sub>): δ = 4.04 (s, 3 H, OCH<sub>3</sub>), 5.18 (s, 2 H, CH<sub>2</sub>Cl), 8.09 (d, *J* = 8.2 Hz, 1H, H<sub>5</sub>), 8.85 (d, *J* = 8.2 Hz, 1 H, H<sub>4</sub>), 9.24 (s, 1 H, H<sub>2</sub>) ppm. <sup>13</sup>C NMR (100 MHz, CDCl<sub>3</sub>): δ = 43.6 (CH<sub>2</sub>Cl), 53.2 (CH<sub>3</sub>O), 124.3 (C<sub>5</sub>), 126.9 (C<sub>3</sub>), 141.5 (C<sub>4</sub>), 147.2 (C<sub>2</sub>), 158.6 (C<sub>6</sub>), 163.8 (C=O) ppm. MS (ESI): *m/z* = 185.9 [M + H]<sup>+</sup>. HRMS (ESI): calcd. for C<sub>8</sub>H<sub>8</sub>ClNO<sub>2</sub> [M + H]<sup>+</sup> 186.0316; found 186.0316; calcd. for C<sub>8</sub>H<sub>8</sub>ClNO<sub>2</sub>Na [M + Na]<sup>+</sup> 208.0136; found 208.0131.

*Synthesis of Methyl 6-[(4,7-dimethyl-1,4,7-triazacyclonon-1-yl)methyl]nicotinate.* Methyl 6-(chloromethyl)nicotinate (95 mg, 0.51 mmol), Me<sub>2</sub>TACN-3HBr (**7**) (205 mg, 0.51 mmol), and anhydrous CH<sub>3</sub>CN (12 mL) were mixed. Then, Na<sub>2</sub>CO<sub>3</sub> (409 mg, 3.85 mmol) and TBABr (8.2 mg, 0.025 mmol) were added, and the mixture was heated at reflux under nitrogen for 20 h. After cooling to room temperature, the resulting yellow mixture was filtered. The filter cake was washed with CH<sub>2</sub>Cl<sub>2</sub> (2 × 5 mL) and the combined filtrates were evaporated under reduced pressure. An aqueous solution of NaOH (1 M, 12 mL) was added to the resulting residue and the mixture was extracted with CH<sub>2</sub>Cl<sub>2</sub> (4 × 15 mL). The combined organic layers were dried over anhydrous MgSO<sub>4</sub>, and the solvent was removed under reduced pressure. Hexane (12 mL) was added to the resulting residue, and the suspension was stirred overnight. The mixture was filtered and the solvent from the yellow filtrates was removed under reduced pressure to yield methyl 6-[(4,7-dimethyl-1,4,7-triazacyclonon-1-yl)methyl]nicotinate as a pale yellow oil (72.3 mg, 46% yield). <sup>1</sup>H NMR (400 MHz, CDCl<sub>3</sub>): δ = 2.36 (s, 6 H, N-CH<sub>3</sub>), 2.65–2.67 (m, 4 H, H<sub>7</sub> or H<sub>8</sub>), 2.76 (s, 4 H, H<sub>9</sub>), 2.82–2.84 (m, 4 H, H<sub>7</sub> or H<sub>8</sub>), 3.91 (s, 2 H, CH<sub>2</sub>), 3.94 (s, 3 H, OCH<sub>3</sub>), 7.61 (dd, *J* = 8.0 and 0.8 Hz, 1 H, H<sub>5</sub>), 8.26 (dd, *J* = 8.0 and 2.0 Hz, 1 H, H<sub>4</sub>), 9.12 (dd, *J* = 2.0 and 0.8 Hz, 1 H, H<sub>2</sub>) ppm. <sup>13</sup>C NMR (100 MHz, CDCl<sub>3</sub>): δ = 46.9 (N-CH<sub>3</sub>), 52.5 (OCH<sub>3</sub>), 56.3 (C<sub>7</sub> or C<sub>8</sub>), 57.2 (C<sub>9</sub>), 57.3 (C<sub>7</sub> or C<sub>8</sub>), 64.7 (CH<sub>2</sub>), 122.9 (C<sub>5</sub>), 124.4 (C<sub>3</sub>), 137.5 (C<sub>4</sub>), 150.4 (C<sub>2</sub>), 165.4 (C<sub>6</sub>), 166.1 (C=O) ppm. MS (ESI): *m/z* = 307.2 [M + H]<sup>+</sup>. HRMS (ESI): calcd. for C<sub>16</sub>H<sub>27</sub>N<sub>4</sub>O<sub>2</sub> [M + H]<sup>+</sup> 307.2129; found 307.2130.

*Synthesis of 6-[(4,7-Dimethyl-1,4,7-triazacyclonon-1-yl)methyl]nicotinic acid (14).* Under ice cooling, an aqueous solution of LiOH (1.6 M, 0.72 mmol) was added dropwise to a solution of methyl 6-[(4,7-dimethyl-1,4,7-triazacyclonon-1-yl)methyl]nicotinate (75 mg, 0.24 mmol) in THF/CH<sub>3</sub>OH (1:1, 1 mL). The reaction was stirred under ice cooling for 30 min and at room temperature for 4.5 h. After this time, the solvent was removed under reduced pressure to afford **14** (62 mg, 87% yield). <sup>1</sup>H NMR (400 MHz, D<sub>2</sub>O): δ = 2.35 (s, 6 H, N-CH<sub>3</sub>), 2.65–2.68 (m, 4 H, H<sub>7</sub> or H<sub>8</sub>), 2.77–2.79 (m, 4 H, H<sub>7</sub> or H<sub>8</sub>), 2.92 (s, 4 H, H<sub>9</sub>), 3.89 (s, 2 H, CH<sub>2</sub>), 7.59 (dd, *J* = 8.0 and 0.4 Hz, 1 H, H<sub>5</sub>), 8.22 (dd, *J* = 8.0 and 2.0 Hz, 1 H, H<sub>4</sub>), 8.88 (dd, *J* = 2.0 and 0.4 Hz, 1 H, H<sub>2</sub>) ppm. MS (ESI): *m/z* = 293.1 [M + H]<sup>+</sup>. HRMS (ESI): calcd. for C<sub>15</sub>H<sub>25</sub>N<sub>4</sub>O<sub>2</sub> [M + H]<sup>+</sup> 293.1972; found 293.1961; calcd. for C<sub>15</sub>H<sub>24</sub>N<sub>4</sub>O<sub>2</sub>Na [M + Na]<sup>+</sup> 315.1791; found 315.1781. <sup>13</sup>C NMR (100 MHz, D<sub>2</sub>O): δ = 44.0 (N-CH<sub>3</sub>), 52.5 (C<sub>7</sub> or C<sub>8</sub>), 53.3 (C<sub>9</sub>), 54.5 (C<sub>7</sub> or C<sub>8</sub>), 61.2 (CH<sub>2</sub>), 123.7 (C<sub>5</sub>), 133.7 (C<sub>3</sub>), 139.2 (C<sub>4</sub>), 151.4 (C<sub>2</sub>), 161.5 (C<sub>6</sub>), 179.7 (C=O) ppm.

*Synthesis of (9a*S*,9b*S*)-5-(Pyrid-2-yl)octahydro-1*H*-dipyrrolo[1,2-*c*:2',1'-*e*]imidazole (15).* Picolinialdehyde (0.34 mL, 3.56 mmol) was added to a solution of (2*S*,2'*S*)-2,2'-bipyrrolidine (0.5 g, 3.56 mmol) in dry Et<sub>2</sub>O (21 mL). The mixture was stirred overnight under nitrogen at room temperature. A small brown precipitate was formed. The reaction mixture was filtered, and the filtrate was concentrated under reduced pressure to give the aminor **15** as yellow oil (0.81 g, 99% yield). *R*<sub>F</sub>: 0.65 AcOEt/CH<sub>3</sub>OH/NH<sub>3</sub>(aq) (5:1:1). <sup>1</sup>H NMR (400 MHz, CDCl<sub>3</sub>): δ = 1.59–1.66 (m, 1 H, H<sub>2</sub>), 1.70–1.90 (m, 6 H, H<sub>2</sub>, H<sub>2'</sub>, 2 × H<sub>3</sub>, 2 × H<sub>3'</sub>), 2.09–2.18 (m, 1 H, H<sub>2'</sub>), 2.29–2.34 (m, 1 H, H<sub>4'</sub>), 2.56–2.62 (m, 2 H, H<sub>4</sub>, H<sub>4'</sub>), 2.93–2.99 (m, 1 H, H<sub>4</sub>), 3.37 (td, *J* = 2.2 and 6.8 Hz, 1 H, H<sub>1'</sub>), 3.42 (td, *J* = 4.8 and 6.8 Hz, 1 H, H<sub>1</sub>), 4.87 (s, 1 H, NCHN), 7.16–7.20 (m, 1 H, pyr-4), 7.61–7.64 (m, 1 H, pyr-2), 7.68 (td, *J* = 1.8 and 7.8 Hz, 1 H, pyr-3), 8.61–8.63 (m, 1 H, pyr-5) ppm. <sup>13</sup>C NMR (100 MHz, CDCl<sub>3</sub>): δ = 24.9, 25.6 (C<sub>3</sub>, C<sub>3'</sub>), 28.9, 30.6 (C<sub>2</sub>, C<sub>2'</sub>), 47.4, 51.9 (C<sub>4</sub>, C<sub>4'</sub>), 70.9, 71.1 (C<sub>1</sub>, C<sub>1'</sub>), 88.2 (NCHN), 122.2 (pyr-2), 122.5 (pyr-4), 136.3 (pyr-3), 149.5 (pyr-5),

159.2 (pyr-1) ppm. MS (ESI):  $m/z = 230.1 [M + H]^+$ . HRMS (ESI): calcd. for  $C_{14}H_{20}N_3 [M + H]^+$  230.1652; found 230.1651; calcd. for  $C_{14}H_{19}N_3Na [M + Na]^+$  252.1471; found 252.1466.

**Synthesis of (2S,2'S)-1-(Pyrid-2-ylmethyl)-2,2'-bipyrrolidine (8).** The aminal **15** (0.35 g, 1.52 mmol) was dissolved in dry  $CH_3OH$  (18 mL, dried over 4 Å molecular sieves) and placed under nitrogen atmosphere. To this solution was added a suspension of  $NaBH_3CN$  (0.11 g, 1.82 mmol) in dry  $CH_3OH$  (25 mL), followed by dropwise addition of TFA (0.23 mL, 3.05 mmol). The reaction mixture was maintained under stirring at room temperature and progress was monitored by TLC. When the reaction was complete,  $NaOH$  (1 M, 25 mL) was added, and the mixture was stirred for 6 h at room temperature. After this time, the product was extracted with  $CH_2Cl_2$  (5 × 15 mL), and the combined organic layers were dried with anhydrous  $MgSO_4$ . The solvent was evaporated under reduced pressure yielding **8** as yellow oil (0.30 g, 86% yield).  $R_f$ : 0.56  $AcOEt/CH_3OH/NH_3(aq)$  (5:1:1).  $^1H$  NMR (400 MHz,  $CDCl_3$ ):  $\delta = 1.37-1.46$  (m, 1 H,  $H_2'$ ), 1.50–1.60 (m, 1 H,  $H_2$ ), 1.69–1.78 (m, 5 H,  $H_2'$ , 2 ×  $H_3$ , 2 ×  $H_3'$ ), 1.89–1.96 (m, 1 H,  $H_2$ ), 2.33–2.41 (m, 1 H,  $H_4$ ), 2.71–2.78 (m, 1 H,  $H_1$ ), 2.81–3.01 (m, 3 H, 2 ×  $H_4'$ ,  $H_4$ ), 3.07 (q,  $J = 9.7$  Hz, 1 H,  $H_1'$ ), 3.63 (d,  $J = 19.1$  Hz, 1 H,  $NCH_2pyr$ ), 4.29 (d,  $J = 19.1$  Hz, 1 H,  $NCH_2pyr$ ), 7.11–7.15 (m, 1 H, pyr-4), 7.39 (d,  $J = 10.2$  Hz, 1 H, pyr-2), 7.62 (td,  $J = 2.4$  and 10.2 Hz, 1 H, pyr-3), 8.50–8.52 (m, 1 H, pyr-5) ppm.  $^{13}C$  NMR (100 MHz,  $CDCl_3$ ):  $\delta = 23.9$ , 24.8 ( $C_3$ ,  $C_3'$ ), 28.2, 28.3 ( $C_2$ ,  $C_2'$ ), 46.4, 55.1 ( $C_4$ ,  $C_4'$ ), 62.5 ( $NCH_2pyr$ ), 63.9, 67.9 ( $C_1$ ,  $C_1'$ ), 121.8 (pyr-4), 122.8 (pyr-2), 136.5 (pyr-3), 149.0 (pyr-5), 160.4 (pyr-1) ppm. MS (ESI):  $m/z = 232.1 [M + H]^+$ . HRMS (ESI): calcd. for  $C_{14}H_{22}N_3 [M + H]^+$  232.1808; found 232.1828; calcd. for  $C_{14}H_{21}N_3Na [M + Na]^+$  254.1628; found 254.1625.

**Synthesis of the Peptidyl Resin Fmoc-Leu-Lys(Boc)-Lys(Boc)-Leu-Rink-MBHA.** This peptidyl resin was synthesized manually by the solid-phase method by using standard Fmoc chemistry starting from an MBHA resin (0.56 mmol/g). The resin was washed before its use with  $CH_3OH$  (2 × 1 min), DMF (2 × 1 min),  $CH_2Cl_2$  (3 × 1 min), TFA/ $CH_2Cl_2$  (1:99, 3 × 1 min), DIPEA/ $CH_2Cl_2$  (1:19, 3 × 1 min),  $CH_2Cl_2$  (3 × 1 min), and DMF (6 × 1 min). Coupling of Fmoc-Rink (4 equiv) was mediated by DIPCDI (4 equiv) and Oxyma (4 equiv) in DMF at room temperature for 5 h. Couplings of Fmoc-amino acids (4 equiv) were performed by using DIPCDI (4 equiv) and Oxyma (4 equiv) in DMF at room temperature for 1 h. Completion of the reactions was monitored by the Kaiser test.<sup>45</sup> Fmoc group removal was achieved with a mixture of piperidine/DMF (3:7, 2 + 10 min). After each coupling and deprotection step, the resin was washed with DMF (6 × 1 min) and  $CH_2Cl_2$  (1 × 1 min). An aliquot of the resulting resin was cleaved with TFA/ $H_2O$ /TIS (95:2.5:2.5) while stirring for 2 h at room temperature. Following TFA evaporation and diethyl ether extraction, the crude peptide was dissolved in  $H_2O$  and lyophilized, affording Fmoc-Leu-Lys-Lys-Leu- $NH_2$  (>99% purity).  $t_R = 7.24$  min (method A). MS (ESI):  $m/z = 361.7 [M + 2H]^{2+}$ , 722.5 [ $M + H$ ]<sup>+</sup>.

**Synthesis of the Peptidyl Resin 10. Conditions a: Conventional Heating.** Resin Fmoc-Leu-Lys(Boc)-Lys(Boc)-Leu-Rink-MBHA (50 mg) was subjected to Fmoc removal and washes as described above to afford peptidyl resin **6**. This resin was placed in a 5 mL round-bottomed flask. Freshly prepared nicotinic acid derivative **5** (10 equiv), COMU (10 equiv), Oxyma (10 equiv), and DIPEA (20 equiv) were dissolved in NMP (1 mL) by sonication and allowed to react for 10 min. This solution was then added to the resin, and the mixture was heated at 80 °C for 72 h under stirring. Then, the resulting resin **10** was washed with NMP (6 × 1 min),  $CH_3OH$  (6 × 1 min), and  $CH_2Cl_2$  (1 × 1 min).

**Conditions b: Microwave Irradiation.** Resin Fmoc-Leu-Lys(Boc)-Lys(Boc)-Leu-Rink-MBHA (50 mg) was subjected to Fmoc removal and washes as described above to afford peptidyl resin **6**. This resin was placed in a 15 mL quartz vial containing a magnetic stir bar. Freshly prepared nicotinic acid derivative **5** (10 equiv), COMU (10 equiv), Oxyma (10 equiv), and DIPEA (20 equiv) were dissolved in NMP (1 mL) by sonication and allowed to react for 10 min. This solution was then added to the reaction vial. The sealed vial was heated at 125 °C under microwave irradiation for 1 h. After the reaction time, upon cooling, the solvent was removed and the resulting

resin **10** was washed with NMP (6 × 1 min),  $CH_3OH$  (6 × 1 min), and  $CH_2Cl_2$  (1 × 1 min).

An aliquot of the resulting resin **10** was cleaved with TFA/ $H_2O$ /TIS (95:2.5:2.5) while stirring for 2 h at room temperature. Following TFA evaporation and diethyl ether extraction, the crude was dissolved in  $H_2O$  and lyophilized, affording peptide derivative **11** (81% purity (conditions a),  $t_R = 5.67$  min (method A); 89% purity (conditions b),  $t_R = 5.75$  min (method A)). MS (ESI):  $m/z = 318.2 [M + 2H]^{2+}$ , 635.4 [ $M + H$ ]<sup>+</sup>.

**Synthesis of the Peptidyl Resin 12.** Peptidyl resin **10** (50 mg) was placed in a syringe and was treated with TBAF (1 M, 664  $\mu$ L) and AcOH (1 M, 20  $\mu$ L) in THF (500  $\mu$ L) under stirring at room temperature for 6 h. After this time, the resin was washed with THF (3 × 1 min),  $CH_3OH$  (3 × 1 min), NMP (3 × 1 min),  $CH_2Cl_2$  (3 × 1 min), and THF (1 × 1 min). The resulting resin was then treated with a solution of LiCl (10 equiv), TsCl (2 equiv), and DIPEA (3 equiv) in THF (1 mL). The reaction mixture was shaken for 8 h at room temperature. This treatment was performed three times. Between treatments and at the end of the reaction, the resin was washed with THF (3 × 1 min),  $CH_3OH$  (3 × 1 min),  $H_2O$  (6 × 1 min), and  $CH_2Cl_2$  (3 × 1 min). An aliquot of the resulting resin **12** was cleaved with TFA/ $H_2O$ /TIS (95:2.5:2.5) while stirring for 2 h at room temperature. Following TFA evaporation and diethyl ether extraction, the crude was dissolved in  $H_2O$  and lyophilized, affording peptide derivative **13** (74% purity).  $t_R = 17.36$  min (method B). MS (ESI):  $m/z = 327.2 [M + 2H]^{2+}$ , 653.4 [ $M + H$ ]<sup>+</sup>.

**Synthesis of the Metal Binding Peptide Conjugate 3.** Peptidyl resin **6** (50 mg) was placed in a 5 mL round-bottomed flask. Then, a solution of **14** (42 mg, 5 equiv), Oxyma (20 mg, 5 equiv), COMU (60 mg, 5 equiv), and DIPEA (48  $\mu$ L, 10 equiv) in NMP was added. The mixture was heated at 80 °C for 48 h. After this time, the resin was washed with NMP (6 × 1 min),  $CH_3OH$  (6 × 1 min), and  $CH_2Cl_2$  (1 × 1 min). Acidolytic cleavage and extractions afforded the trifluoroacetate salt of the metal binding peptide **3**<sub>TFA</sub>. Next, **3**<sub>TFA</sub> was purified and basified by flash column chromatography using  $CH_2Cl_2/CH_3OH/NH_3(aq)$  (200:20:2) as mobile phase. The amount of  $NH_3(aq)$  was gradually increased up to  $CH_2Cl_2/CH_3OH/NH_3(aq)$  (200:20:5). Fractions containing the desired compound were combined, and the solvent was removed under reduced pressure providing the free amine metal binding peptide **3** (>99% purity).  $t_R = 6.12$  min (method A).  $^1H$  NMR (400 MHz,  $CD_3OD+D_2O$ ):  $\delta = 0.75-0.89$  (m, 12 H, 4 ×  $CH_3(\delta)$ -Leu), 1.29–1.77 (m, 18 H), 2.52 (s, 6 H), 2.62–2.77 (m, 12 H), 2.89–2.92 (m, 4 H), 3.94 (s, 2 H), 4.18–4.28 (m, 4 H), 7.39 (d,  $J = 8.2$  Hz, 1 H,  $H_c$ ), 8.13 (dd,  $J = 2.2$  and 8.2 Hz, 1 H,  $H_b$ ), 8.93 (d,  $J = 2.2$  Hz, 1 H,  $H_a$ ) ppm. MS (ESI):  $m/z = 387.8 [M + 2H]^{2+}$ , 774.6 [ $M + H$ ]<sup>+</sup>. HRMS (ESI): calcd. for  $C_{39}H_{73}N_{11}O_5 [M + 2H]^{2+}$  387.7893; found 387.7884; calcd. for  $C_{39}H_{72}N_{11}O_5 [M + H]^+$  774.5712; found 774.5701.

**Synthesis of the Metal Binding Peptide Conjugate 4.** A 15 mL quartz vial containing a magnetic stir bar was charged with peptidyl resin **12** (50 mg). Then, a solution of **8** (13.5 mg, 2 equiv), NaI (0.2 mg, 0.04 equiv) and DIPEA (120  $\mu$ L, 24 equiv) in NMP was added to the reaction vial. The sealed vial was heated at 125 °C under microwave irradiation for 1 h. After the reaction time, upon cooling, the solvent was removed and the resulting resin was washed with NMP (6 × 1 min),  $CH_3OH$  (6 × 1 min), and  $CH_2Cl_2$  (1 × 1 min). The resulting resin was cleaved with TFA/ $H_2O$ /TIS (95:2.5:2.5) while stirring for 2 h at room temperature. Following TFA evaporation and diethyl ether extraction, the crude was dissolved in  $H_2O$  (5 mL) and extracted with  $CH_2Cl_2$  (6 × 3 mL). The aqueous phase was then lyophilized, affording the metal binding peptide **4**<sub>TFA</sub>. Reverse-phase column chromatography eluting with  $H_2O/CH_3CN$  (89:11) afforded pure **4**<sub>TFA</sub> (>99% purity).  $t_R = 5.77$  min (method A). Next, **4**<sub>TFA</sub> was dissolved in  $CH_2Cl_2/CH_3OH/NH_3(aq)$  (200:20:2). Flash column chromatography was performed using  $CH_2Cl_2/CH_3OH/NH_3(aq)$  (200:20:2) as the mobile phase. The amount of  $NH_3(aq)$  was gradually increased up to  $CH_2Cl_2/CH_3OH/NH_3(aq)$  (200:20:5). Fractions containing the desired compound were combined, and the solvent was removed under reduced pressure providing the free amine metal binding peptide **4**.  $^1H$  NMR (400 MHz,  $CD_3OD+D_2O$ ):  $\delta = 0.90-$

1.02 (m, 12 H, 4 × CH<sub>3</sub>(δ)-Leu), 1.28–1.89 (m, 24 H), 2.24–2.33 (m, 2 H), 2.76 (t, *J* = 7.3 Hz, 4 H, 2 × CH<sub>2</sub>(ε)-Lys), 2.98–3.25 (m, 4 H), 3.54–3.62 (m, 2 H), 4.17–4.40 (m, 8 H), 7.25–7.28 (m, 1 H, H<sub>e</sub>), 7.48 (d, *J* = 7.8 Hz, 1 H, H<sub>g</sub>), 7.60 (d, *J* = 8 Hz, 1 H, H<sub>c</sub>), 7.74–7.78 (m, 1 H, H<sub>e</sub>), 8.19 (d, *J* = 8 Hz, 1 H, H<sub>b</sub>), 8.39–8.40 (m, 1 H, H<sub>d</sub>), 8.87 (s, 1 H, H<sub>a</sub>) ppm. MS (ESI): *m/z* = 424.7 [M + 2H]<sup>2+</sup>, 848.6 [M + H]<sup>+</sup>. HRMS (ESI): calcd. for C<sub>45</sub>H<sub>75</sub>N<sub>11</sub>O<sub>5</sub> [M + 2H]<sup>2+</sup> 424.7971; found 424.7974; calcd. for C<sub>45</sub>H<sub>74</sub>N<sub>11</sub>O<sub>5</sub> [M + H]<sup>+</sup> 848.5869; found 848.5882.

**Synthesis of Metallotetrapeptide 1<sub>Zn</sub>** [Zn(OTf)<sub>2</sub>(Me<sub>2</sub>PyTACN)-LKKL-NH<sub>2</sub>]. A solution of Zn(CF<sub>3</sub>SO<sub>3</sub>)<sub>2</sub> (4.70 mg, 0.012 mmol) in CH<sub>3</sub>CN (0.5 mL) was added dropwise to a vigorously stirred solution of the metal binding peptide 3 (10 mg, 0.012 mmol) in CH<sub>3</sub>CN (1 mL). After a few seconds, the cloudy solution became completely brown and clear. The reaction mixture was stirred at room temperature for 5 h. After this time, the solution was filtered through Celite, and diethyl ether (25 mL) was added upon which a precipitate was formed. In a few days, the solvent was decanted and the solid was dried *in vacuo* to give the metalloprotein 1<sub>Zn</sub> as a light brown powder (9.7 mg, 66% yield). <sup>1</sup>H NMR (400 MHz, CD<sub>3</sub>OD+D<sub>2</sub>O): δ = 0.73–0.86 (m, 12 H, 4 × CH<sub>3</sub>(δ)-Leu), 1.32–1.73 (m, 18 H), 2.20–2.30 (m, 2 H), 2.47 (s, 6 H), 2.68–2.80 (m, 12 H), 2.97–3.01 (m, 2 H), 4.16–4.24 (m, 6 H), 7.54 (d, *J* = 8.0, 1 H, H<sub>c</sub>), 8.34 (dd, *J* = 2.0 and 8.0 Hz, 1 H, H<sub>c</sub>), 9.04 (bs, 1 H, H<sub>a</sub>) ppm. HRMS (ESI): calcd. for C<sub>39</sub>H<sub>73</sub>ClN<sub>11</sub>O<sub>5</sub>Zn [M - (CF<sub>3</sub>SO<sub>3</sub>)<sub>2</sub> + Cl + 2H]<sup>3+</sup> 292.1577; found 292.1596; calcd. for C<sub>40</sub>H<sub>73</sub>ClF<sub>3</sub>N<sub>11</sub>O<sub>8</sub>ZnS [M - CF<sub>3</sub>SO<sub>3</sub> + Cl + 2H]<sup>2+</sup> 511.7143; found 511.7148.

**Synthesis of Metallotetrapeptide 1<sub>Cu</sub>** [Cu(OTf)<sub>2</sub>(Me<sub>2</sub>PyTACN)-LKKL-NH<sub>2</sub>]. The same protocol described for 1<sub>Zn</sub> was followed but using a solution of Cu(CF<sub>3</sub>SO<sub>3</sub>)<sub>2</sub> (4.67 mg, 0.012 mmol). 1<sub>Cu</sub> was obtained as a light blue powder (10.8 mg, 74% yield). HRMS (ESI) calcd for C<sub>39</sub>H<sub>71</sub>ClCuF<sub>6</sub>N<sub>11</sub>O<sub>5</sub> [M - (CF<sub>3</sub>SO<sub>3</sub>)<sub>2</sub> + Cl]<sup>+</sup> 871.4570; found 871.4575; calcd for C<sub>40</sub>H<sub>71</sub>CuF<sub>3</sub>N<sub>11</sub>O<sub>8</sub>S [M - CF<sub>3</sub>SO<sub>3</sub>]<sup>+</sup> 985.4418; found 985.4420; calcd for C<sub>41</sub>H<sub>72</sub>CuF<sub>6</sub>N<sub>11</sub>O<sub>11</sub>S<sub>2</sub> [M + H]<sup>+</sup> 1135.4013; found 1135.4015.

**Synthesis of Metallotetrapeptide 2<sub>Zn</sub>** [Zn(OTf)<sub>2</sub>(BPBP)-LKKL-NH<sub>2</sub>]. The same protocol described for 1<sub>Zn</sub> was followed, but using the metal binding peptide 4 (10 mg, 0.011 mmol). 2<sub>Zn</sub> was obtained as a light brown powder (9.1 mg, 64% yield). <sup>1</sup>H NMR (400 MHz, CD<sub>3</sub>OD + D<sub>2</sub>O): δ = 0.90–1.04 (m, 12 H, 4 × CH<sub>3</sub>(δ)-Leu), 1.45–2.21 (m, 26 H), 2.45–2.53 (m, 2 H), 2.76–2.83 (m, 2 H), 2.86–2.95 (m, 4 H, 2 × CH<sub>2</sub>(δ)-Lys), 3.11–3.14 (m, 2 H), 4.16–4.42 (m, 6 H), 4.57 (bb), 7.59 (d, *J* = 8 Hz, 1 H, H<sub>g</sub>), 7.62–7.66 (m, 1 H, H<sub>e</sub>), 7.68 (d, *J* = 8.2, 1 H, H<sub>c</sub>), 8.12 (dt, *J* = 1.5 and 7.8 Hz, 1 H, H<sub>f</sub>), 8.49 (dd, *J* = 2.0 and 8.2 Hz, 1 H, H<sub>b</sub>), 8.79 (d, *J* = 4.9 Hz, 1 H, H<sub>d</sub>), 9.20 (bb, 1 H, H<sub>a</sub>) ppm. HRMS (ESI): calcd. for C<sub>46</sub>H<sub>75</sub>F<sub>3</sub>N<sub>11</sub>O<sub>8</sub>SZn [M - CF<sub>3</sub>SO<sub>3</sub> + 2H]<sup>3+</sup> 354.1583; found 354.1580; calcd. for C<sub>46</sub>H<sub>74</sub>F<sub>3</sub>N<sub>11</sub>O<sub>8</sub>SZn [M - CF<sub>3</sub>SO<sub>3</sub> + H]<sup>2+</sup> 530.7338; found 530.7324; calcd. for C<sub>47</sub>H<sub>75</sub>F<sub>6</sub>N<sub>11</sub>O<sub>11</sub>S<sub>2</sub>Zn [M + 2H]<sup>2+</sup> 605.7137; found 605.7141.

**Synthesis of Metallotetrapeptide 2<sub>Cu</sub>** [Cu(OTf)<sub>2</sub>(BPBP)-LKKL-NH<sub>2</sub>]. The same protocol described for 1<sub>Zn</sub> was followed but using a solution of Cu(CF<sub>3</sub>SO<sub>3</sub>)<sub>2</sub> (4.67 mg, 0.011 mmol) and the metal binding peptide 4 (10 mg, 0.011 mmol). 2<sub>Cu</sub> was obtained as a light blue powder (9.3 mg, 65% yield). HRMS (ESI): calcd. for C<sub>45</sub>H<sub>74</sub>CuN<sub>11</sub>O<sub>5</sub> [M - (CF<sub>3</sub>SO<sub>3</sub>)<sub>2</sub> + H]<sup>3+</sup> 303.8385; found 303.8403; calcd. for C<sub>46</sub>H<sub>74</sub>CuF<sub>3</sub>N<sub>11</sub>O<sub>8</sub>S [M - CF<sub>3</sub>SO<sub>3</sub> + H]<sup>2+</sup> 530.2340; found 530.2360; calcd. for C<sub>47</sub>H<sub>75</sub>CuF<sub>6</sub>N<sub>11</sub>O<sub>11</sub>S<sub>2</sub> [M + 2H]<sup>2+</sup> 605.2139; found 605.2161.

**DNA Binding Assays.** The competition assay was undertaken with fixed DNA and competitor (EB) concentrations and variable conjugates. Fluorescence measurements were performed on a Varian Cary Eclipse spectrofluorophotometer using a 1 cm quartz cell at room temperature. The DNA–EB complexes were excited at 546 nm, and the fluorescence was measured at 595 nm. To the solution of EB and DNA (10 mM Tris pH 7.2, 1.3 μM EB, and 3.9 μM DNA) were added aliquots of a 1 mM stock solution of the conjugates and the fluorescence was measured after each addition until the fluorescence was reduced to 50%. The apparent binding constants (*K*<sub>app</sub>) for conjugates were calculated from *K*<sub>EB</sub> × [EB] = *K*<sub>app</sub> × [drug], where [EB] is the concentration of EB (1.3 μM), [drug] is the concentration

of conjugates at a 50% reduction of fluorescence and *K*<sub>EB</sub> is known (*K*<sub>EB</sub> = 1 × 10<sup>7</sup> M<sup>-1</sup> for ct-DNA; 9.5 × 10<sup>6</sup> M<sup>-1</sup> for poly(dA-dT)<sub>2</sub>, and 9.9 × 10<sup>6</sup> M<sup>-1</sup> for poly(dG-dC)<sub>2</sub>).<sup>46</sup>

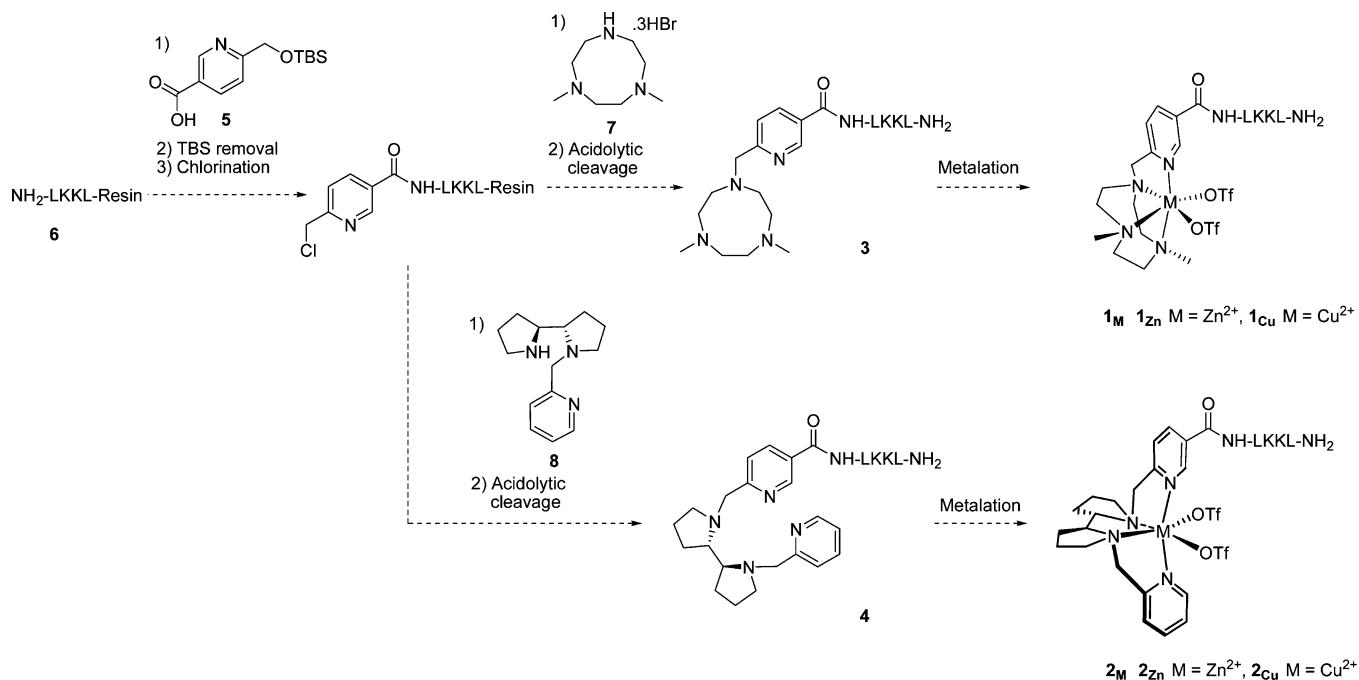
**DNA Cleavage Experiments.** DNA cleavage studies were monitored by agarose gel electrophoresis. The pUC18 plasmid DNA was used at concentration of 0.5 μg·μL<sup>-1</sup> (1512 μM nucleotides; 756 μM bp). Stock solutions were freshly prepared in milli-Q water. Reactions were performed by mixing 0.5 μL of supercoiled pUC18 DNA, appropriate aliquots of ligand, metal binding peptide conjugate or metal salt concentration and 1 μL of solution of sodium L-ascorbate (1.96 mM) in a 1.5 fold excess relative to the compound concentration (when required). Solution of sodium L-ascorbate was freshly prepared prior to each experiment. Then, appropriate amount of Cacodylate buffer (0.1 M, pH 6) or TE buffer (10 mM Tris, 1 mM EDTA, pH 7.4) was added to complete 20 μL total volume. The final concentrations of pUC18 DNA was 37.8 μM in nucleotides (18.9 μM bp). The samples were incubated at 37 °C during the appropriate time. Then, the reactions were quenched by adding a buffer solution (6 μL) consisting of bromophenol blue (0.25%), xylene cyanol (0.25%), and glycerol (30%) and loaded on 0.8% agarose gel in 0.5 × TBE buffer (0.045 M Tris, 0.045 M boric acid and 1 mM EDTA) at 125 V for 1.5 h. Afterward, the agarose gel was revealed with an ethidium bromide (10 mg/mL in TBE) for 30 min and the bands were visualized on a capturing system (ProgRes CapturePro 2.7). To test the presence of reactive oxygen species (ROS) and to explore the DNA interaction sites, different scavengers and groove binders were added to the reaction mixtures. The ROS scavengers used were Tiron (10 mM) and DMSO (3 μL). To explore the possible selectivity of DNA cleavage, the major groove binder methyl green (20 μM) and the minor groove binder Hoechst (20 μM) were included in the reaction mixtures. ROS scavengers and groove binders were freshly prepared prior to each experiment. Samples were treated as described above. The proportion of different forms of pUC18 plasmid DNA was analyzed by comparing the relative intensity of each band by the total intensities of all bands in the lane using software ImageJ. All experiments were performed at least twice.

**DNA Kinetics.** The kinetic studies of the DNA cleavage were performed with plasmid pUC18, which was incubated at 37 °C with 1<sub>Cu</sub>, 2<sub>Cu</sub>, [Cu(PyTACN)]<sup>2+</sup> and [Cu(BPBP)]<sup>2+</sup> (15 μM, 1.5-fold excess of sodium L-ascorbate). Samples were treated as described above, aliquots were taken at specific times, and quenched by placing them on ice and adding a buffer solution (6 μL) consisting of bromophenol blue (0.25%), xylene cyanol (0.25%), and glycerol (30%).<sup>47</sup> Time-dependent concentrations of supercoiled (Form I) and nicked DNA (Form II) were fit to a first-order consecutive model defined by eq 1 where *C* corresponds to the respective % plasmid DNA form at time *t* (min), *C*<sub>0</sub> corresponds to the initial concentration of plasmid DNA and *k*<sub>obs</sub> corresponds to the observed first-order rate constant (expressed as min<sup>-1</sup>). All kinetic experiments were performed at least in triplicate.

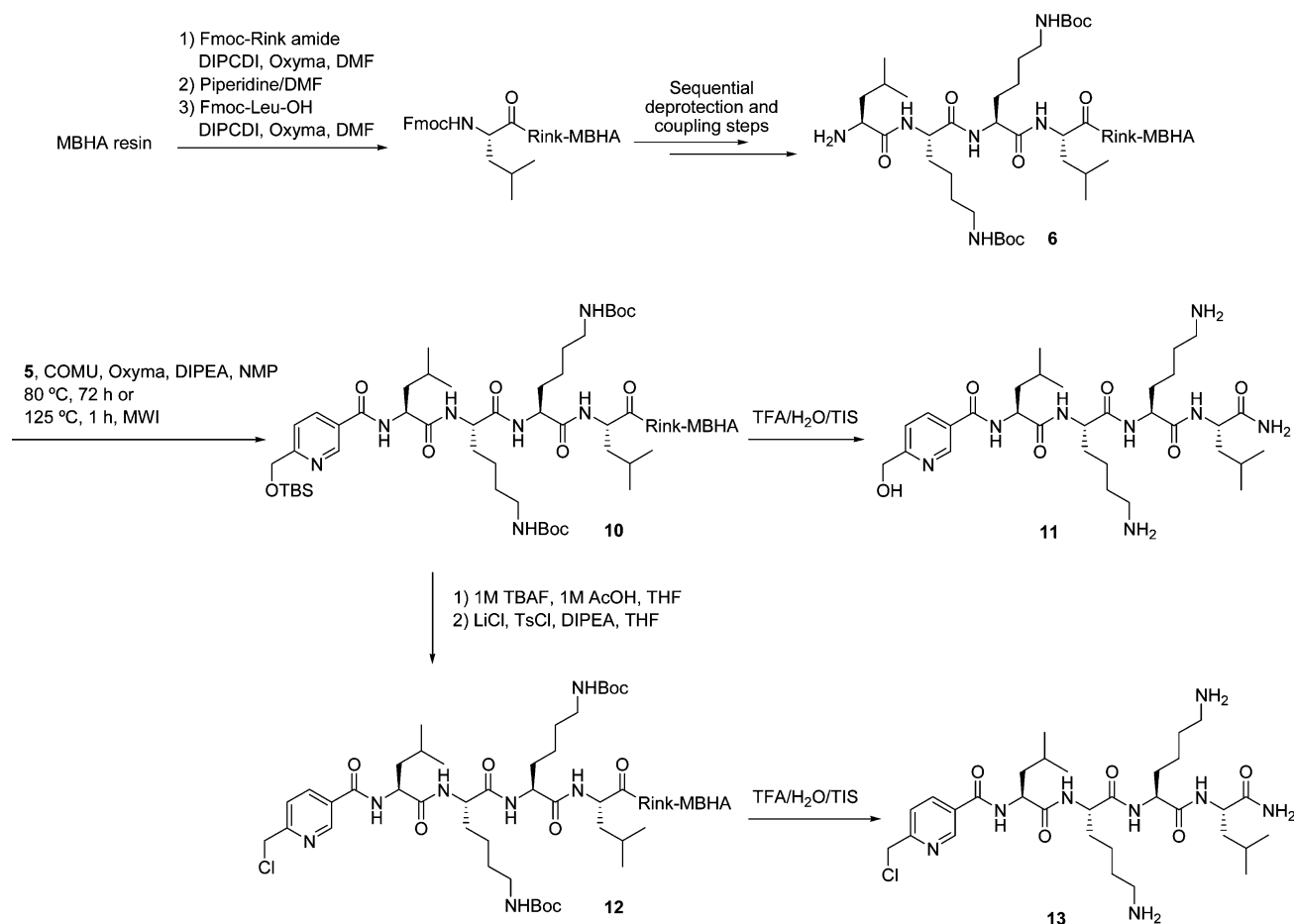
$$C = C_0 \exp(-k_{\text{obs}} t) \quad (1)$$

**Cleavage of 158bp Fragment.** Supercoiled pSP73 plasmid was digested with *Nde* I restriction endonuclease and 3'-end-labeled by treatment with Klenow exo<sup>-</sup> and [α-<sup>32</sup>P]-deoxy-ATP. After radioactive labeling, the DNA first cleaved with *Nde* I was still digested with *Hind* III to yield a 158 and 2306 base pair fragments. The 158 bp fragment was purified by 1% agarose gel electrophoresis and isolated from the gel by Promega Wizard SV Gel cleanup system.

A 9 μL solution containing 20 mM Tris-HCl (pH 7.2) or 50 mM sodium cacodylate (pH 6), DNA (2.5 × 10<sup>-4</sup> M per base), and desired conjugate was incubated for 15 min at room temperature. Cleavage was initiated by the addition of 1 μL of 1 mM sodium L-ascorbate and allowed to react for 1 h at 37 °C. An aliquot of 1.5 μL of 3 M sodium acetate buffer (pH 5.2) and 0.1 mM EDTA were then added, and samples were precipitated with 150 μL of ethanol. Pellets were rinsed twice with 150 μL of ethanol, lyophilized, and resuspended in a formamide loading buffer. DNA cleavage products were resolved by polyacrylamide (PAA) gel electrophoresis under denaturing conditions (13%/8 M urea PAA gel).

Scheme 1. Synthetic Strategy for the Preparation of the Metallotetrapeptides  $1_M$  and  $2_M$ 

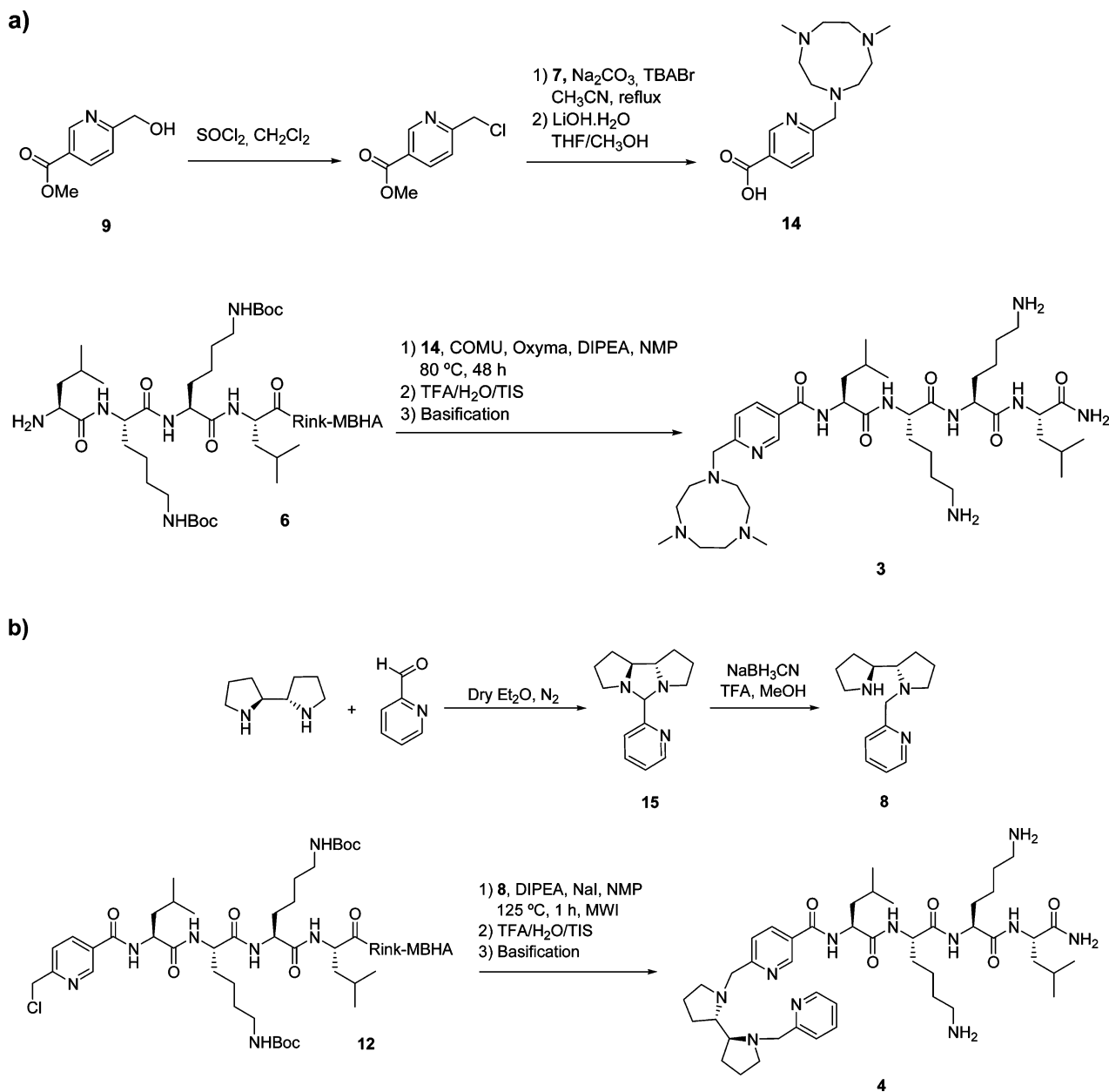
Scheme 2. Synthesis of the Peptidyl Resin 12



**Cell Lines.** Human MCF-7 breast cancer and CAPAN-1 pancreatic cancer cell lines were obtained from the American Type Culture Collection (ATCC, Rockville, MD, USA). 1BR3G transformed human

skin fibroblasts were from the European Collection of Cell Cultures (ECACC, Porton, UK). Cells were maintained in Dulbecco's modified Eagle's medium (DMEM) supplemented with 10% fetal bovine serum

Scheme 3. (a) Synthesis of the Metal Binding Peptide Conjugate 3 and (b) Synthesis of the Metal Binding Peptide Conjugate 4



and 100 U/mL penicillin-streptomycin, all from GIBCO BRL (Grand Island, NY, USA), at 37 °C under a humidified atmosphere containing 5% CO<sub>2</sub>.

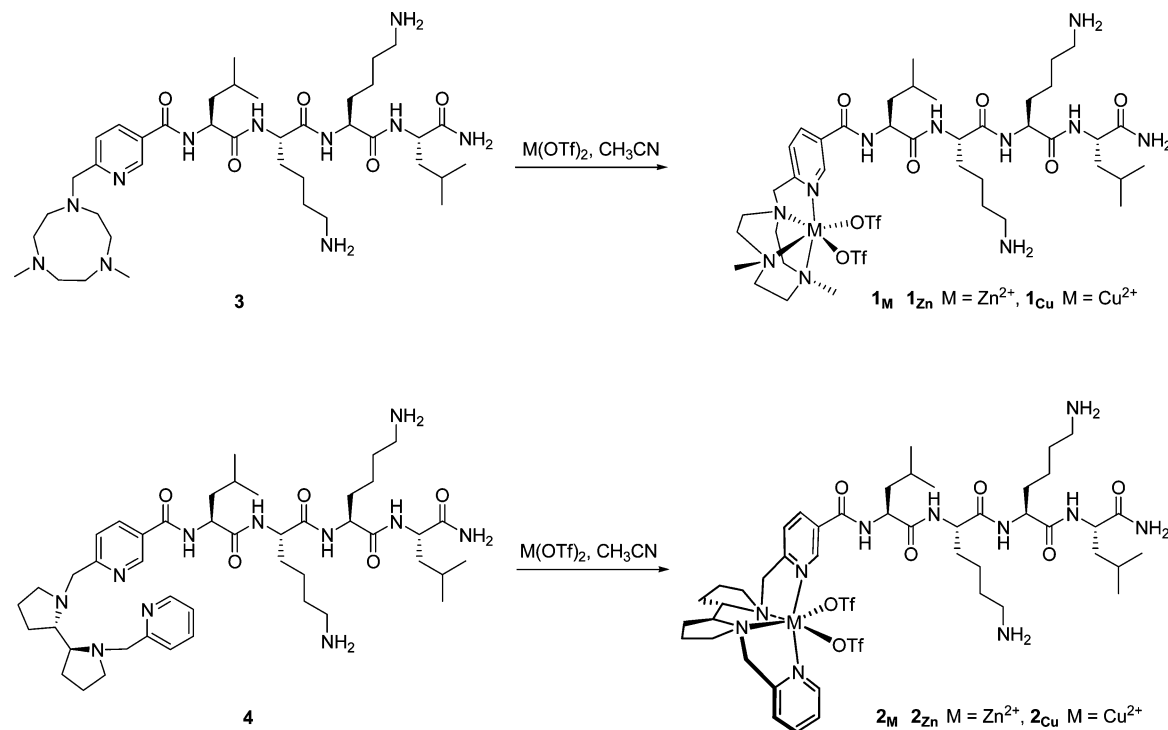
**Cytotoxicity Assays.** The cytotoxic activity of the compounds in MCF-7, CAPAN-1, and 1BR3G cells was determined by the MTT reduction assay. Aliquots of 5000 1BR3G cells, 6000 MCF-7 cells, or 10 000 CAPAN-1 cells were seeded onto flat-bottomed 96-well plates. 24 h later, the cells were treated for 48 h with the compounds at concentrations ranging from 0 to 100 μM. After removal of the treatment, the cells were washed with PBS and incubated for 2 additional hours with 100 μL of fresh culture medium together with 10 μL of MTT (Sigma-Aldrich). The medium was discarded and DMSO (Sigma-Aldrich) was added to each well to dissolve the purple formazan crystals. Plates were agitated at room temperature for 2 min and the absorbance of each well was determined with an absorbance microplate reader (ELx800, BioTek, Winooski, USA) at a wavelength of 570 nm. Three replicates for each treatment were tested. The cell viability was determined as a percentage of the control untreated cells, by dividing the mean absorbance of each treatment by the mean absorbance of the untreated cells. The concentration that reduces by

50% the cell viability (IC<sub>50</sub>) was established for each compound using a four-parameter curve fit (Gen5 Data Analysis Software, BioTeck).

**Hemolysis.** The hemolytic activity of the compounds at 25, 100, and 150 μmol/L was evaluated by determining hemoglobin release from erythrocyte suspensions of fresh human blood (5% vol/vol) as previously described.<sup>48</sup>

## RESULTS AND DISCUSSION

The synthesis of the metallotetrapeptides of general structure **1<sub>M</sub>** and **2<sub>M</sub>**, containing the <sup>Me</sup>PyTACN and (*S,S'*)-BPBP ligands, respectively, was planned through the solid-phase synthesis of the corresponding metal binding peptide conjugate **3** or **4** and subsequent metalation in solution (Scheme 1). These metal binding peptide conjugates were prepared following a synthetic strategy adapted from a previous work<sup>43,44</sup> and involved: (i) attachment of the nicotinoyl derivative **5** to the N-terminus of the tetrapeptidyl resin **6**, (ii) *tert*-butyldimethylsilyl (TBS) group removal, (iii) chlorina-

Scheme 4. Synthesis of the Metallotetrapeptides  $1_M$  and  $2_M$ 

tion, and (iv) alkylation with the corresponding secondary amine **7** or **8**.

**Solid-Phase Synthesis of the Metal Binding Peptides **3** and **4**.** We first studied the synthesis of the metal binding peptide **3**. A 4-methylbenzhydrylamine (MBHA) polystyrene resin was used as solid support. After Fmoc-Rink linker coupling with *N,N'*-diisopropylcarbodiimide (DIPCDI) and ethyl 2-cyano-2-(hydroxyimino)acetate (Oxyma) in DMF, the tetrapeptidyl resin **6** was prepared following a 9-fluorenylmethoxycarbonyl (Fmoc)/*tert*-butyl (*t*Bu) strategy by sequential deprotection and coupling steps under standard conditions (Scheme 2). Fmoc group was removed by treatment with piperidine/NMP (3:7), and couplings of the conveniently protected Fmoc-amino acids were mediated by DIPCDI and Oxyma in DMF.

With the peptidyl resin **6** in hand, we set out to examine the conjugation of the nicotinoyl derivative **5** (Scheme 2). This compound was prepared from the commercially available dimethylpyridine-2,5-dicarboxylate through selective reduction of the ester at position 2 affording methyl 6-(hydroxymethyl)-nicotinate (**9**). Subsequent protection of the primary alcohol with a *tert*-butyldimethylsilyl (TBS) group and saponification of the methyl ester provided **5** in 52% overall yield. The conjugation of **5** to the peptidyl resin **6** was optimized under conventional heating and under microwave irradiation. Using the former method, best conditions involved treatment of **6** with the nicotinoyl derivative **5** (10 equiv), 1-[(1-(cyano-2-ethoxy-2-oxoethylideneaminoxy) dimethylaminomorpholino)] uronium hexafluorophosphate (COMU) (10 equiv), Oxyma (10 equiv), and *N,N'*-diisopropylethylamine (DIPEA) (20 equiv) in NMP at 80 °C for 72 h. Cleavage of an aliquot of the resulting peptidyl resin **10** with trifluoroacetic acid (TFA)/H<sub>2</sub>O/triisopropylsilane (TIS) yielded the expected peptide derivative **11** in 81% purity. The use of the same reaction

conditions under microwave irradiation at 125 °C reduced the reaction time to 1 h, leading to **11** in 89% purity.

After successful incorporation of the nicotinoyl derivative **5**, the silyl ether group was converted into chloride in two steps (Scheme 2). Thus, resin **10** was treated with a mixture of 1 M tetrabutylammonium fluoride (TBAF) and 1 M AcOH in THF for 6 h to remove the TBS group. Chlorination of the resulting hydroxyl group was carried out with LiCl (10 equiv), *p*-toluenesulfonyl chloride (TsCl) (2 equiv), and DIPEA (3 equiv) in THF for 8 h. This treatment was performed three times to ensure complete conversion to the chloride. Success of these two steps was confirmed by HPLC and ESI-MS analysis of the crude reaction mixture obtained after acidolytic cleavage of an aliquot of the resulting resin **12**. Peptide derivative **13** was obtained in 74% purity.

Next, we attempted the *N*-alkylation of resin **12** with Me<sup>2</sup>TACN (**7**) under microwave irradiation at 125 °C for 1 h. After acidolytic cleavage, NMR analysis showed that the trifluoroacetate salt of the metal binding peptide **3** (**3**<sub>TFA</sub>) was obtained together with a byproduct that could not be identified. Thus, an alternative route was assayed in order to obtain **3** in higher purity which was based on the coupling of 6-[(4,7-dimethyl-1,4,7-triazacyclonon-1-yl)methyl]nicotinic acid (**14**) to the tetrapeptidyl resin **6** (Scheme 3a). The nicotinic acid derivative **14** was prepared through chlorination of **9**, alkylation with the secondary amine **7**, and final saponification. Thus, **14** was obtained in 34% overall yield and was characterized by ESI-MS, HRMS and NMR. Next, the coupling of compound **14** (5 equiv) to peptidyl resin **6** was mediated by COMU (5 equiv), Oxyma (5 equiv) and DIPEA (10 equiv) in NMP at 80 °C for 48 h. After acidolytic cleavage and basification by column chromatography eluting with CH<sub>2</sub>Cl<sub>2</sub>/CH<sub>3</sub>OH/NH<sub>3(aq)</sub>, the metal binding peptide **3** was obtained in >99% purity. The effectiveness of the removal of trifluoroacetate counterions was checked by <sup>19</sup>F-NMR (see Figures S18 and S19 in the

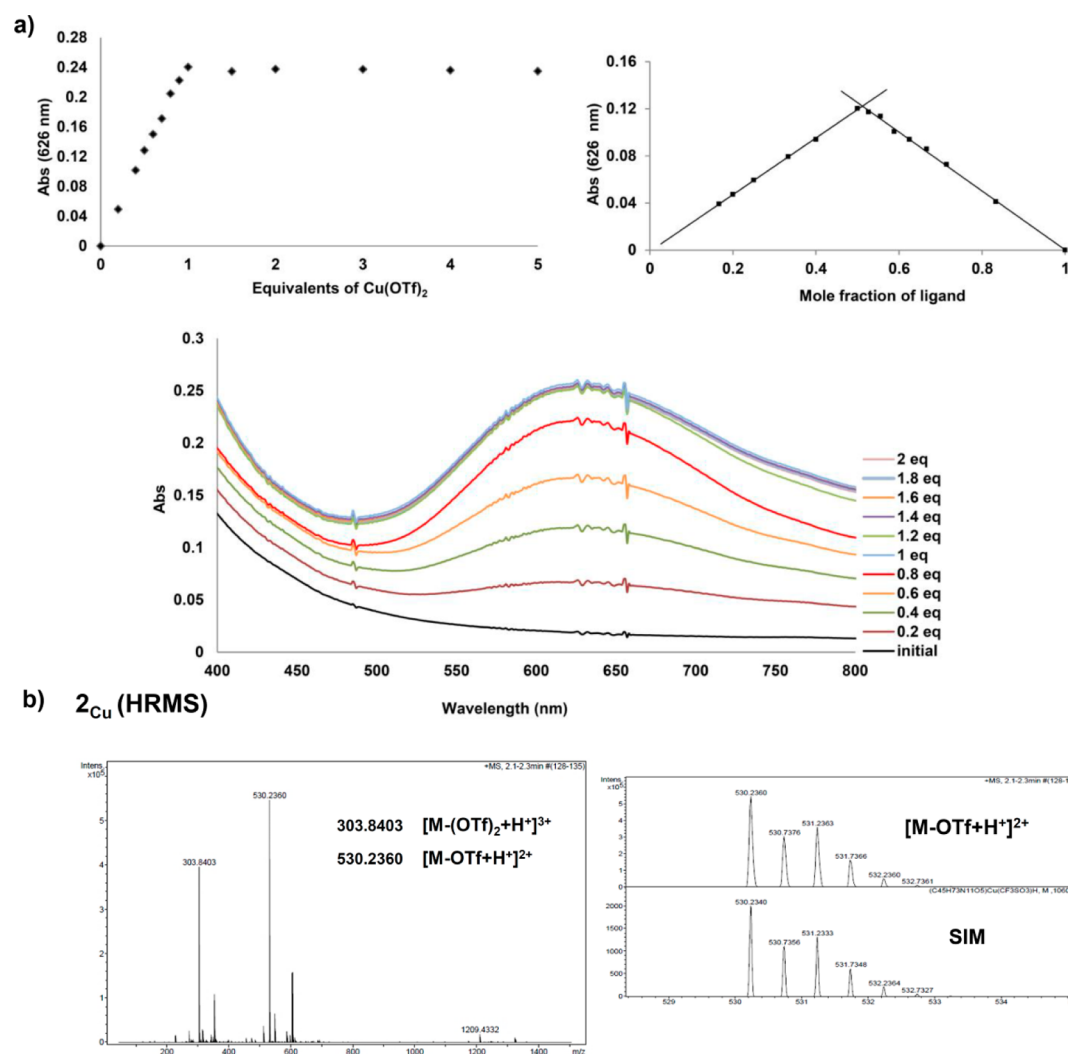


**Figure 1.** (a) UV–vis spectrophotometric titration of the metal binding peptide **4** (2 mM) with  $\text{Cu}(\text{OTf})_2$  (40 mM) in  $\text{CH}_3\text{OH}$  at 25 °C. Job's plot of absorbance at 626 nm verifies the 1:1 stoichiometry between **4** and  $\text{Cu}(\text{OTf})_2$ . (b) Observed HRMS for  $2\text{Cu}$  with the theoretical isotopic patterns. Full spectra are collected in the [Supporting Information](#).

**SI).**Compound **3** was fully characterized by ESI-MS, HRMS, and NMR.

The synthesis of the metal binding peptide **4** was assayed by alkylation of the peptidyl resin **12** with the secondary amine **8** under microwave irradiation at 125 °C for 1 h. ([Scheme 3b](#)). Compound **8** was prepared by first reacting (*S,S'*)-bipyrrolidine with picolylaldehyde followed by reduction of the aminal **15** with  $\text{NaBH}_3\text{CN}$  in the presence of TFA in  $\text{CH}_3\text{OH}$ , and was obtained in 85% overall yield.<sup>49</sup> Alkylation of resin **12** with **8** and subsequent acidolytic cleavage and basification afforded **4** in >99% purity. Analysis by ESI-MS, HRMS, and NMR showed the presence of the expected metal binding peptide.

**Synthesis of the Metallotetrapeptides  $1_M$  and  $2_M$ .** Once we obtained aminopyridine peptide conjugates **3** and **4**, we assayed their binding to metal triflate salts (zinc and copper, [Scheme 4](#)). Reactions were carried out by dissolving **3** or **4** in  $\text{CH}_3\text{CN}$  followed by addition of a solution of the corresponding metal triflate in  $\text{CH}_3\text{CN}$ . The mixture was stirred at room temperature for 5 h. Subsequent filtration through Celite and precipitation with diethyl ether yielded metallotetrapeptides  $1_M$  and  $2_M$  as powders which were characterized by HRMS.

**Characterization of the Metallotetrapeptides  $1_M$  and  $2_M$ .** Metallopeptides  $1_{\text{Cu}}$ ,  $1_{\text{Zn}}$ ,  $2_{\text{Cu}}$  and  $2_{\text{Zn}}$  were characterized by high resolution mass spectrometry, UV–vis and  $^1\text{H}$  NMR spectroscopy, when possible.

First, the stoichiometry of the reaction between metal binding peptide conjugate **4** and  $\text{Cu}(\text{II})$  was studied by performing a UV–vis spectrophotometric titration. Sequential addition of 0.2 equiv of  $\text{Cu}(\text{OTf})_2$  to a solution of **4** in  $\text{CH}_3\text{OH}$  revealed that a maximum absorbance at 626 nm, characteristic of the  $\text{Cu}^{2+}$  d-d transition, was reached upon addition of 1 equiv of the metal salt ([Figure 1](#)). The formation of  $2_{\text{Cu}}$  was clearly appreciable by the blue color of the solution. Further addition of  $\text{Cu}(\text{OTf})_2$  up to 5 equiv did not elicit changes in the maximum absorbance. In addition, in order to further ensure the role of the tetradentate ligand as unique metal binding site, a titration of the Fmoc deprotected tetrapeptide (devoid of the tetradentate ligand) with  $\text{Cu}(\text{OTf})_2$  was performed. No significant absorbance was observed in the UV–vis spectrum. The sum of the experiments strongly suggests that Lys side chains are excluded from metal coordination and the chelation occurs only with the (*S,S'*)-BPBP ligand located at the N-terminus of the peptide. Furthermore, Job plot of absorbance at  $\lambda_{\text{max}}$  of the titration vs the mole fraction of **4** confirmed the 1:1

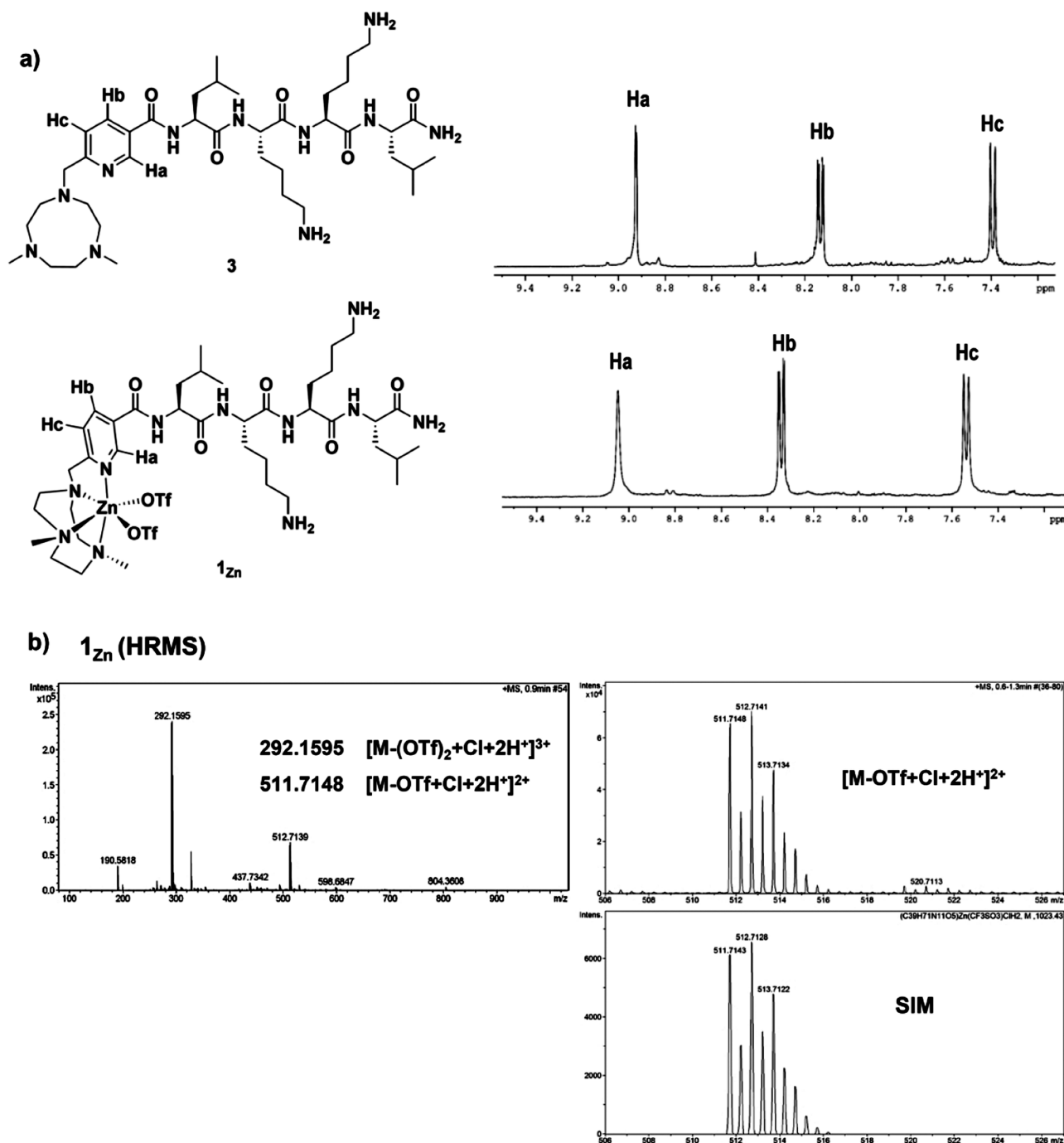


**Figure 2.** (a) <sup>1</sup>H NMR (selected aromatic region, CD<sub>3</sub>OD) of **3** and metallopeptide **1<sub>Zn</sub>**. (b) HRMS for **1<sub>Zn</sub>** with the theoretical isotopic patterns. Full spectra analyses are collected in the [Supporting Information](#).

complexation stoichiometry. On the other hand, metal binding to **3** was also investigated by UV–vis, supporting also the 1:1 complexation stoichiometry to form **1<sub>Cu</sub>** (Figure S20). UV–vis spectrophotometric titrations for the formation of **1<sub>Cu</sub>** and **2<sub>Cu</sub>** showed a linear correlation between the absorbance of their respective d-d band and the amount of Cu(OTf)<sub>2</sub> added. This linearity demonstrates that **3** and **4** bind Cu<sup>2+</sup> ions with a high binding constant (*K<sub>a</sub>*), for which a lower limit of 10<sup>8</sup> M<sup>-1</sup> is deduced. Therefore, we conclude that the cationic nature of the peptide does not decrease the binding ability of the polyamine ligand, at least to a detectable level reachable by the UV–vis titrations.

Finally, the HRMS spectrum of **2<sub>Cu</sub>** showed cluster ions at *m/z* 605.2161 and 530.2360 with isotopic patterns that can be assigned to [M+2H<sup>+</sup>]<sup>2+</sup> and [M-OTf+H<sup>+</sup>]<sup>2+</sup> ions (Figure 1 and SI). Likewise, the HRMS spectrum of **1<sub>Cu</sub>** also displayed cluster ions at *m/z* 985.4420 and 871.4575 with isotopic patterns consistent with [M-OTf]<sup>+</sup> and [M-(OTf)<sub>2</sub>+Cl]<sup>+</sup> formulation (Figure S20 and SI). Peaks that could be assigned to Cu:metallopeptide stoichiometries different from 1:1 were not observed in the spectra, further confirming the proposal derived from UV–vis titrations, that each peptide molecule binds a single metal ion, at the aminopyridine site.

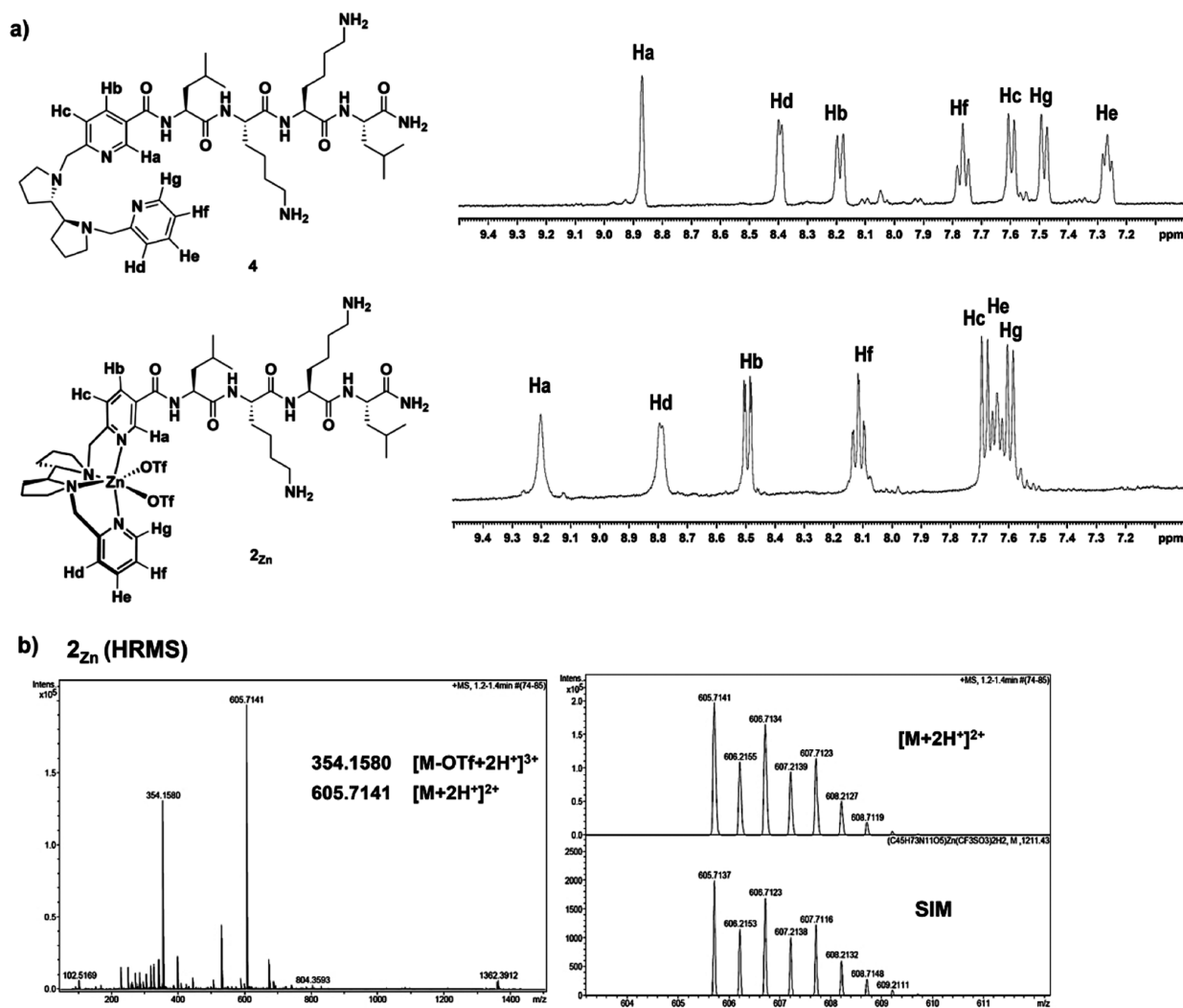


**Table 1.** Apparent DNA Binding Constants ( $K_{\text{app}}$ ) ( $\times 10^6 \text{ M}^{-1}$ ) Evaluated for Conjugates 3, 4,  $1_{\text{Cu}}$ , and  $2_{\text{Cu}}$ 

compound	ct-DNA	poly(dA-dT) <sub>2</sub>	poly(dG-dC) <sub>2</sub>
3	0.27	n/a	n/a
4	0.13	n/a	n/a
$1_{\text{Cu}}$	7.1	6.2	5.7
$2_{\text{Cu}}$	5.9	5.3	4.7

demonstrates that, upon chelation, the metal complex in both cases binds more strongly to the DNA. This could be attributed to the two labile positions that contain the metallic center, which may be engaged in covalent interactions with the phosphates of DNA, along with electrostatic interactions between the positively charged metal ion and the negatively charged phosphates. On the other hand,  $1_{\text{Cu}}$  and  $2_{\text{Cu}}$  exhibit slightly higher binding affinity for random ct-DNA than for poly(dA-dT)<sub>2</sub> and poly(dG-dC)<sub>2</sub> containing regular alternating purine and pyrimidine sequences. Small differences in binding affinities of  $1_{\text{Cu}}$  and  $2_{\text{Cu}}$  to poly(dA-dT)<sub>2</sub> and poly(dG-dC)<sub>2</sub> indicate low sequence selectivity. In all cases,  $1_{\text{Cu}}$  displaces EB from all studied DNAs a bit more efficiently than  $2_{\text{Cu}}$ .

**DNA Cleavage Experiments.** The DNA cleavage abilities of Me<sub>2</sub>PyTACN and (S,S′)-BPBP ligands, conjugates 3, 4,  $1_{\text{Zn}}$ ,  $1_{\text{Cu}}$ ,  $2_{\text{Zn}}$ , and  $2_{\text{Cu}}$  were screened with pUC18 plasmid DNA. The conversion of supercoiled plasmid DNA (Form I) to nicked circular DNA (Form II) and linear DNA (Form III) was monitored by using agarose gel electrophoresis.

As shown in Figure S21, we first studied the activity of metal-free systems as well as in the presence of Zn<sup>2+</sup> or Cu<sup>2+</sup> in a 1:1 ratio with the Me<sub>2</sub>PyTACN and (S,S′)-BPBP ligands or their peptide conjugates 3 and 4 in order to form in situ the resulting metallopeptides  $1_{\text{Zn}}$ ,  $1_{\text{Cu}}$ ,  $2_{\text{Zn}}$ , and  $2_{\text{Cu}}$ . To avoid any effect due to the participation of metal ions, 1 mM EDTA was added as chelating agent in metal-free cleavage tests.

Both tetradentate ligands and conjugate 3 and 4 were able to moderately interact with the supercoiled DNA (Form I) at moderate concentrations and short reaction times (50 μM, 1 h; Figure S21, lanes 2 and 3). The same results were obtained when Zn<sup>2+</sup> and Cu<sup>2+</sup> metal ions were added in the respective reactions (Figure S21, lanes 4–7). Taking into account that the hydrolysis of the phosphodiester linkage in DNA is a difficult reaction, the appearance of these bands may result from unwinding of the DNA. Remarkably, in both series the addition of sodium L-ascorbate (Asc) as reducing agent in Cu<sup>2+</sup> complexes (1:1.5 ratio, M:Asc) promoted the total conversion of the supercoiled DNA (Form I) to nicked and linear DNA (Forms II and III, respectively), followed by smeared bands due to the DNA fragmentation (Figure S21, lanes 8 and 9). Thus, these extensive complete DNA transformations clearly indicated the importance of Cu<sup>2+</sup> and sodium L-ascorbate in the redox-active cleavage mechanism.<sup>11</sup> See Table S1 for the quantification of the DNA bands.

To further examine the results observed by the different metal-free systems, typical ROS scavengers for superoxide radical O<sub>2</sub><sup>•−</sup> (Tiron) and hydroxyl radical ·OH (DMSO) were included in these assays. As depicted in Figure S22, the DNA band promoted by conjugates 3 and 4 did not disappear when incubated in the presence of ROS scavengers. This observation suggests that ROS species were not involved in these metal-free assays. Moreover, in Figure S22 the appearance of an additional band between Form I and Form II was evidenced in all cases. This could be attributed to a close interaction of conjugates 3 and 4 with DNA leading to a less compact intermediate form, previous to the nicked form (Form II). It should be noted that metal-free and Zn<sup>2+</sup> experiments were slightly more efficient at acidic pH 6 than at neutral pH 7.4 (Figures S21 and S23), suggesting that their interaction abilities depended on their protonation form<sup>11,47,50</sup> despite being incubated for longer periods (24 h).<sup>51–53</sup>

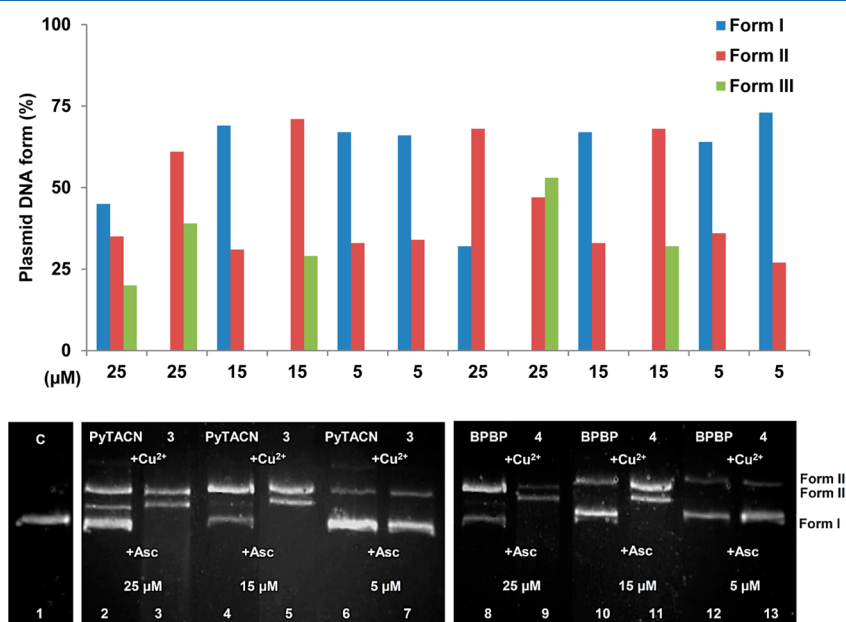


**Figure 4.** Representative comparative assays of pUC18 DNA (18.9 μM (bp)) incubated with Me<sub>2</sub>PyTACN, (S,S′)-BPBP, 3, or 4 at different concentrations in Cacodylate buffer (0.1 M, pH 6) at 37 °C for 1 h. Cu<sup>2+</sup> was added in a 1:1 (M:L) ratio. C = DNA control. Asc = sodium L-ascorbate (1:1.5, M:Asc). The bottom panel shows the agarose gel images; the top panel shows the relative proportion of plasmid DNA (Form I, Form II and Form III). All lanes were run in the same gel. The relative proportion of the different bands is provided in the Supporting Information (Table S2).

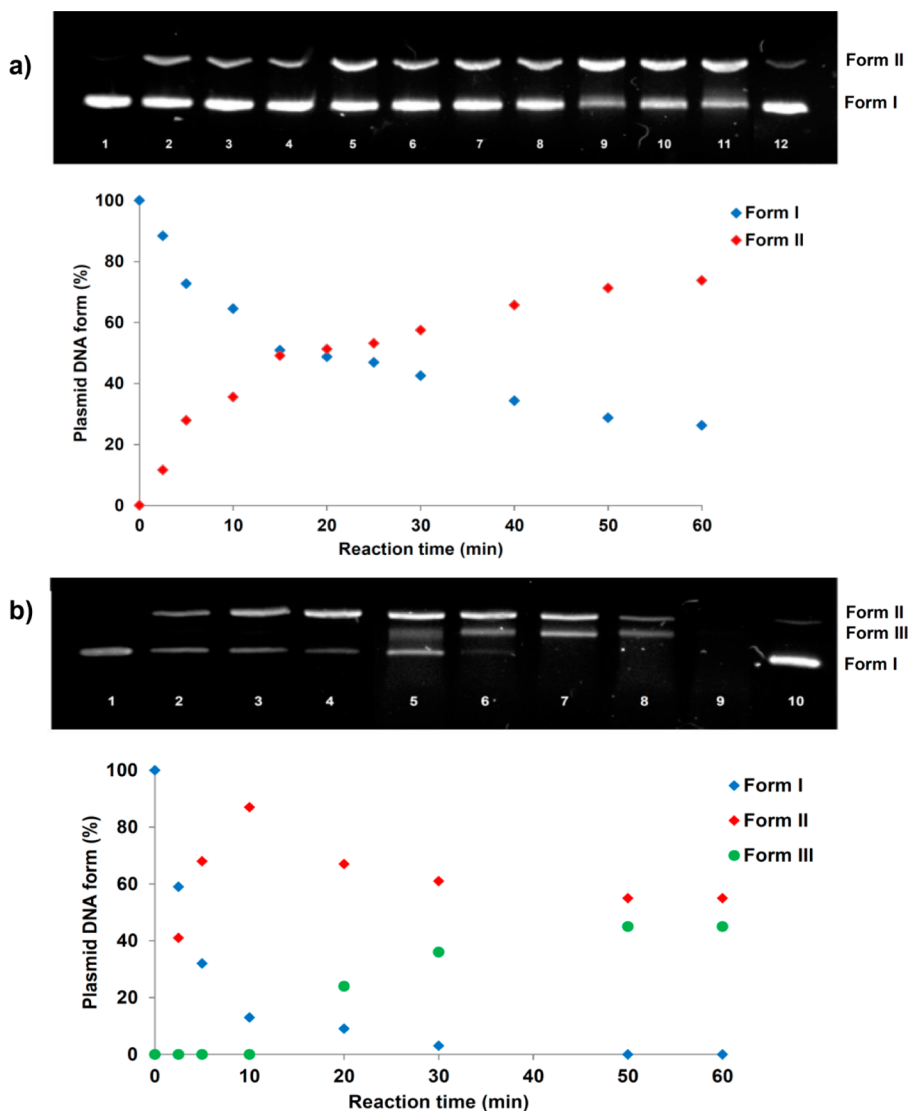


**Figure 5.** (a) Kinetic trace of nicked pUC18 DNA (18.9  $\mu\text{M}$  (bp)) promoted by incubating  $[\text{Cu}(\text{BPBP})]^{2+}$  (15  $\mu\text{M}$ ) in Cacodylate buffer (0.1 M, pH 6) at 37  $^{\circ}\text{C}$ .  $\text{Cu}^{2+}$  was added in a 1:1 (M:L) and sodium L-ascorbate (Asc) (1:1.5, M:Asc). Top panel shows the agarose gel images at different reaction times: 0 min (lane 1), 2.5 min (lane 2), 5 min (lane 3), 10 min (lane 4), 15 min (lane 5), 20 min (lane 6), 30 min (lane 7), 50 min (lane 8), 60 min (lane 9), 90 min (lane 10), 90 min (lane 11) and DNA control at 90 min (lane 12). Bottom panel represents the variation of the relative proportion of plasmid DNA (Form I, Form II). (b) Kinetics of nicked pUC18 DNA (18.9  $\mu\text{M}$  (bp)) promoted by incubating  $2_{\text{Cu}}$  (15  $\mu\text{M}$ ) in Cacodylate buffer (0.1 M, pH 6) at 37  $^{\circ}\text{C}$ .  $\text{Cu}^{2+}$  was added in a 1:1 (M:L) and Asc (1:1.5, M:Asc). Top panel shows the agarose gel images at different reaction times: 0 min (lane 1), 2.5 min (lane 2), 5 min (lane 3), 10 min (lane 4), 20 min (lane 5), 30 min (lane 6), 50 min (lane 7), 60 min (lane 8), 90 min (lane 9) and DNA control at 90 min (lane 10). Bottom panel represents the variation of the relative proportion of plasmid DNA (Form I, Form II and Form III).

Encouraged by these results, we examined the concentration dependence of both compound series in an effort to determine the optimal cleavage conditions and the tetrapeptide involvement during the cleavage reaction. Therefore, compounds **3**, **4**,  $1_{\text{Zn}}$ , and  $2_{\text{Zn}}$  were tested at higher concentrations (100, 150, and 200  $\mu\text{M}$ ) in Cacodylate buffer for 1 h. However, in all cases the interaction with DNA and the subsequent band formation was not improved (data not shown). On the other hand, the cleavage systems for the metallopeptides  $1_{\text{Cu}}$  and  $2_{\text{Cu}}$  and their respective ligands were examined at lower concentrations (25, 15, and 5  $\mu\text{M}$ ). Notably,  $[\text{Cu}(\text{PyTACN})]^{2+}$  (Figure 4, lanes 2 and 4) and  $[\text{Cu}(\text{BPBP})]^{2+}$  (Figure 4, lanes 8 and 10) complexes were not able to totally cleave the plasmid DNA while their copper metallopeptides, under the same reaction conditions, displayed excellent nuclease activities at 25 and 15

$\mu\text{M}$ . As depicted in Figure 4 (lanes 5 and 11), the total conversion of the supercoiled form (Form I) to the nicked and linear form (Form II and Form III, respectively) were readily detected when incubating the copper metallopeptides at both concentrations in the presence of sodium L-ascorbate. At the lowest concentration (5  $\mu\text{M}$ ), the metallopeptides only showed a weak interaction with the supercoiled form of DNA. Furthermore, control assays of supercoiled plasmid DNA using (*S,S'*)-BPBP (50  $\mu\text{M}$ ) and **4** (25  $\mu\text{M}$ ) and 10% excess of both binding moieties were performed (see Figure S24 and Figure S25, lanes 10–12). Remarkably, in both cases the Cu complexes ( $[\text{Cu}(\text{BPBP})]^{2+}$  and  $2_{\text{Cu}}$ ) using 10% excess of the ligand showed the same activities as previously observed in 1:1 (M:L) ratio. This observation clearly ruled out the presence of free Cu and its involvement in the oxidative cleavage reaction.

Additionally, the oxidative cleavage mechanisms promoted by compounds  $[\text{Cu}(\text{PyTACN})]^{2+}$ ,  $[\text{Cu}(\text{BPBP})]^{2+}$ ,  $\mathbf{1}_{\text{Cu}}$  and  $\mathbf{2}_{\text{Cu}}$  at 25 and 15  $\mu\text{M}$  were found to be almost inhibited at neutral pH 7.4 (Figure S26). These results revealed that the conjugation of  $[\text{Cu}(\text{PyTACN})]^{2+}$  and  $[\text{Cu}(\text{BPBP})]^{2+}$  complexes to this cationic tetrapeptide sequence clearly improved their nuclease abilities, highlighting a promising peptide contribution to the DNA cleavage. Inhibition at neutral pH also suggests that the cationic nature of the peptide is lost or at least attenuated in these conditions. Lysine side chains are expected to have a  $\text{pK}_a \sim 10.5$ , but deprotonation at neutral pH may be rationalized by the close proximity of positive charge from the metal cation and additional lysine groups in the peptide.

In order to define and quantify the impact of introducing the cationic tetrapeptide sequence to  $[\text{Cu}(\text{PyTACN})]^{2+}$  and  $[\text{Cu}(\text{BPBP})]^{2+}$  complexes on DNA cleavage efficiency, different kinetic studies of pUC18 DNA degradation were carried out. The loss of supercoiled DNA and the enhanced levels of open circular and linear forms were quantified after gel electrophoresis, as described in the Experimental Section, and further fitted with the aid of the kinetic model. Experimental reaction conditions were carefully optimized with the aim of monitoring the gradual disappearance of the supercoiled DNA (Form I). Bearing in mind that we were not able to properly follow the cleavage of supercoiled DNA incubating  $\mathbf{2}_{\text{Cu}}$  at 25  $\mu\text{M}$  (Figure S27) or at 10  $\mu\text{M}$  (Figure S28), a compound concentration of 15  $\mu\text{M}$  was fixed for all kinetic assays. Hence, the time course of the supercoiled plasmid DNA cleavage (Form I) into nicked form (Form II) promoted by  $[\text{Cu}(\text{PyTACN})]^{2+}$ ,  $[\text{Cu}(\text{BPBP})]^{2+}$ , and their corresponding metalloproteins  $\mathbf{1}_{\text{Cu}}$  and  $\mathbf{2}_{\text{Cu}}$ , respectively, are shown in Figures 5 and Figure S29. First we observed that the rate of conversion from Form I to Form II induced by  $[\text{Cu}(\text{BPBP})]^{2+}$  at 15  $\mu\text{M}$  increased with the increased reaction time (Figure Sa). The extension of the supercoiled DNA cleavage varied exponentially with the reaction time rendering pseudo first-order kinetics with an apparent initial first-order rate constant ( $k_{\text{obs}}$ ) of  $\sim 0.027 \text{ min}^{-1}$  and a half-life time ( $t_{1/2}$ ) of  $\sim 25.7 \text{ min}$  (Figure S30). Even extending the reaction time until 90 min (Figure Sa, lane 11), no linear DNA (Form III) was formed, which was supported by the previous behavior observed by  $[\text{Cu}(\text{BPBP})]^{2+}$  at the same concentration (Figure 4). Nevertheless, when performing the same experiment incubating  $\mathbf{2}_{\text{Cu}}$  at 15  $\mu\text{M}$  (Figure Sb), we were pleased to observe that this metalloprotein totally cleaved the supercoiled DNA in the initial stage of the reaction (15–30 min, Figure Sb lanes 5–7). Moreover, subsequent nicking mediated by  $\mathbf{2}_{\text{Cu}}$  promoted the conversion to nicked and linear forms (Figure Sb, lanes 7 and 8), finally yielding the entire degradation of DNA after 90 min of reaction (Figure Sb, lane 9). The  $k_{\text{obs}}$  for  $\mathbf{2}_{\text{Cu}}$  was found to be  $\sim 0.11 \text{ min}^{-1}$  with  $t_{1/2} \approx 6.4 \text{ min}$  (Figure S30). These results evidenced that the DNA cleavage activity promoted by the metalloprotein  $\mathbf{2}_{\text{Cu}}$  gave  $\sim 4$ -fold rate acceleration over that of compound  $[\text{Cu}(\text{BPBP})]^{2+}$ , in agreement with the previous studies shown in Figure 4.

On the other hand, the same kinetic study was performed for  $[\text{Cu}(\text{PyTACN})]^{2+}$  and  $\mathbf{1}_{\text{Cu}}$  under the same reaction conditions (Figure S29a and S29b). Remarkably, the kinetic profile found for  $[\text{Cu}(\text{PyTACN})]^{2+}$  contrasted with the findings for the metalloprotein  $\mathbf{1}_{\text{Cu}}$ . The reaction profile observed for  $[\text{Cu}(\text{PyTACN})]^{2+}$  pointed out a very slow cleavage activity after 90 min, displaying a pseudo first-order kinetic behavior with  $k_{\text{obs}} \sim 0.0071 \text{ min}^{-1}$  and  $t_{1/2} \sim 97.6 \text{ min}$  for supercoiled DNA (Figure S29a and Figure S30). However, its corresponding metal-

loprotein  $\mathbf{1}_{\text{Cu}}$  showed a pseudo first-order cleavage rate similar to  $\mathbf{2}_{\text{Cu}}$  (Figure S29b) and was able to mediate the cleavage of the supercoiled DNA in the very early stage of the reaction (10–15 min, lanes 4 and 5). This metalloprotein displayed  $k_{\text{obs}}$  of  $\sim 0.16 \text{ min}^{-1}$  with a supercoiled DNA  $t_{1/2} \approx 4.3 \text{ min}$ , which corresponded to a  $\sim 23$ -fold rate enhancement of the DNA cleavage process over the parent complex  $[\text{Cu}(\text{PyTACN})]^{2+}$  (Figure S30). Remarkably, the results obtained correlated to the cleavage profiles previously found for  $[\text{Cu}(\text{PyTACN})]^{2+}$  and  $\mathbf{1}_{\text{Cu}}$ , depicted in Figure 4.

Therefore, the large rate enhancement of the DNA cleavage activity promoted by the two metalloproteins  $\mathbf{1}_{\text{Cu}}$  and  $\mathbf{2}_{\text{Cu}}$  made evident that, at very low concentrations, the conjugation of  $[\text{Cu}(\text{PyTACN})]^{2+}$  and  $[\text{Cu}(\text{BPBP})]^{2+}$  complexes to the cationic tetrapeptide sequence LKKL contributed very favorably to the DNA cleavage activity. Notably, this positive effect was specially noted when comparing the DNA cleavage activity observed for  $[\text{Cu}(\text{PyTACN})]^{2+}$  and its corresponding metalloprotein  $\mathbf{1}_{\text{Cu}}$ .

Studies toward the identification of the oxidizing species involved in the oxidative cleavage mechanism promoted by  $[\text{Cu}(\text{BPBP})]^{2+}$  and  $\mathbf{2}_{\text{Cu}}$  were undertaken. We considered the possibility that either reactive oxygen species (ROS) or a metal based oxidant such as copper-superoxide or copper peroxide species will be responsible for the oxidative damage. ROS scavengers for superoxide radical  $\text{O}_2^-$  (Tiron) and hydroxyl radical  $\cdot\text{OH}$  (DMSO) were added in the cleavage assays (Figure 6, see Table S3 for the quantification of the DNA bands). The concentration of  $(S,S')$ -BPBP ligand was fixed at 50  $\mu\text{M}$  while for  $\mathbf{4}$  was incubated at its optimal cleavage conditions (15  $\mu\text{M}$ , Figure 4, lane 11). Notably, an important cleavage inhibition was detected for  $[\text{Cu}(\text{BPBP})]^{2+}$  and  $\mathbf{2}_{\text{Cu}}$  when Tiron was added in the reaction systems. In contrast,

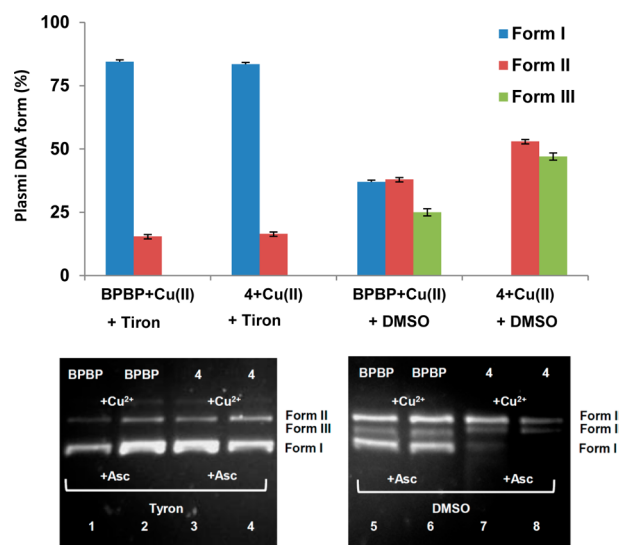


**Figure 6.** Agarose gel images of pUC18 DNA (18.9  $\mu\text{M}$  (bp)) incubating  $(S,S')$ -BPBP (50  $\mu\text{M}$ ) and  $\mathbf{4}$  (15  $\mu\text{M}$ ) with ROS inhibitors in Cacodylate buffer (0.1 M, pH 6) at 37  $^{\circ}\text{C}$  for 1 h. ROS inhibitors: Tiron (10 mM) and DMSO (3  $\mu\text{L}$ ).  $\text{Cu}^{2+}$  was added in a 1:1 (M:L) ratio. Asc = sodium L-ascorbate (1:1.5, M:Asc). The bottom panel shows the agarose gel images; the top panel shows the relative proportion of plasmid DNA (Form I, Form II and Form III). Representative data from two independent experiments expressed as mean  $\pm$  standard deviation. All lanes were run in the same gel. The relative proportion of the different bands is depicted in Table S3.

both compounds exhibited high nuclease chemistry despite of the presence of DMSO as hydroxyl radical inhibitor. These results evidenced that both systems generate the superoxide radical. Therefore, we assumed that these species may be the responsible for the oxidative DNA cleavage. A caution note must be made at this point regarding the possible implication of metal based oxidation species. ROS scavengers are highly reactive against diffusible species, and it is highly unlikely that they would efficiently react with a putative metal based oxidant (such as a copper-superoxide species) that is placed in close proximity to the DNA oxidative target by virtue of its interaction with the peptide moiety. Therefore, inhibition of the oxidative damage by the ROS scavenger Tiron strongly suggests that diffusible superoxide anion is responsible for the oxidation activity.

In order to assess whether the enhanced nuclease reactivity of the copper metallopeptides is reflecting an enhanced binding affinity or groove preference toward plasmid DNA, further cleavage experiments with  $[\text{Cu}(\text{BPBP})]^{2+}$  and  $2_{\text{Cu}}$  were performed in the presence of major groove or minor groove DNA inhibitors. The same concentrations as in the previous study were used. As shown in Figure 7, the cleavage activity of

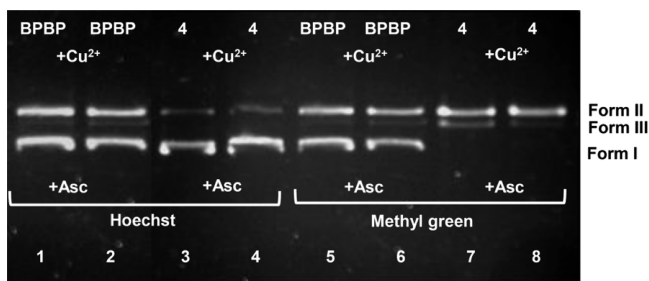


**Figure 7.** Agarose gel images of pUC18 DNA (18.9  $\mu\text{M}$  (bp)) incubating BPBP (50  $\mu\text{M}$ ) and 4 (15  $\mu\text{M}$ ) in the presence of DNA minor groove inhibitor Hoechst (20  $\mu\text{M}$ ) and major groove inhibitor Methyl green (20  $\mu\text{M}$ ) in Cacodylate buffer (0.1 M, pH 6) at 37  $^{\circ}\text{C}$  for 1 h.  $\text{Cu}^{2+}$  was added in a 1:1 (M:L) ratio. Asc = Sodium L-Ascorbate (1:1.5, M:Asc). All lanes were run in the same gel.

$[\text{Cu}(\text{BPBP})]^{2+}$  was partially inhibited in the presence of the major groove-binding agent methyl green. The same effect was observed when Hoechst was incubated in the reaction as minor groove binding agent. This result proposed that the chemical nuclease activity of  $[\text{Cu}(\text{BPBP})]^{2+}$  was partially inhibited in both cases, suggesting that this oxidative complex was not able to selectively cleave the plasmid DNA. Interestingly, when analyzing the same experiments incubating the  $2_{\text{Cu}}$  metallopeptide, no inhibition effect on the DNA cleavage was observed in the presence of major groove inhibitor methyl green. In contrast, the presence of Hoechst induced a complete inhibition of the nuclease activity provided by  $2_{\text{Cu}}$ , proposing that this minor-groove intercalator might bind in the preferred binding sites of conjugate  $2_{\text{Cu}}$ . These data suggested an improved binding affinity to the DNA minor groove by this conjugate and is in total agreement with the minor groove orientation induced by other previously reported cationic tetrapeptide sequences.<sup>31,33</sup> The LKKL sequence might preferentially interact in the minor-groove region by non-covalent interactions involving the protonated lysine  $\epsilon\text{-NH}_3^+$  groups.

In order to obtain further information on ability of  $1_{\text{Cu}}$  and  $2_{\text{Cu}}$  to produce sequence-selective DNA cleavage, the 158 bp

*Hind* III/*Nde* I restriction fragment of the plasmid pSP73 was mixed with various concentrations of metal-binding peptide conjugates 3 and 4 previously metalated with 1 equiv of  $\text{Cu}^{2+}$ . The cleavage reaction was triggered by addition of 100  $\mu\text{M}$  sodium L-ascorbate. Samples were analyzed by PAGE. Figures S31 and S32 show the results obtained for the reactions carried out in 20 mM Tris-HCl (pH 7.2) and 50 mM cacodylate buffer (pH 6). The copper metallopeptides  $1_{\text{Cu}}$  and  $2_{\text{Cu}}$  led to a nonspecific cleavage pattern where the DNA fragment was randomly cleaved at all nucleotides. The DNA was less cleaved by  $1_{\text{Cu}}$  than by  $2_{\text{Cu}}$ . Our results suggest that both conjugates do not exhibit sequence-specific binding to the DNA. On the other hand, previous experiments have demonstrated that the cleavage mechanism is based on the production of ROS species, predominantly superoxide radical. In aqueous solutions the mean lifetime of superoxide radical is 50 ms and the diffusion distance 320 nm.<sup>54</sup> Thus, this species can diffuse along the double helix and induce strand scission at relatively great distance from the site of production.

Finally, the biological activity of the compounds 3, 4,  $1_{\text{Zn}}$ ,  $1_{\text{Cu}}$ ,  $2_{\text{Zn}}$ , and  $2_{\text{Cu}}$  was assayed against nonmalignant cells (1BR3G). It was found that none of these compounds exhibited any cytotoxicity (>100  $\mu\text{M}$ ). Further assays against MCF-7 and CAPAN-1 cancer cell lines showed that all compounds were also found not to be cytotoxic in these cases (Figure S34). Additionally, the same compounds displayed very low hemolytic activities even at 150  $\mu\text{M}$  (Table S4). The biological data suggests that these metallopeptides are not capable of reaching the cell nucleus. However, despite this preliminary cellular behavior, we envision that the conjugation of the same redox-active moieties and metal complexes to a functional peptide vector may render a potential strategy from a therapeutic point of view. Further efforts are currently underway toward achieving an effective cellular delivery with peptide-based carriers, while improving the intracellular accumulation and redox-directed anticancer effects.

## CONCLUSIONS

In the present work, the conjugation feasibility of Cu and Zn complexes to the short cationic tetrapeptide LKKL by means of solid-phase peptide synthesis (SPPS) has been studied. A straightforward methodology to render novel metal binding peptide conjugates has been successfully developed, and subsequent metalation of  $\text{Me}_2\text{PyTACN}$  and (*S,S'*)-BPBP-based peptides with Zn(II) and Cu(II) metal ions has been fully characterized by HRMS, NMR, and UV-vis. DNA cleavage studies under optimized conditions indicate that copper metallopeptides based on  $\text{Me}_2\text{PyTACN}$  and (*S,S'*)-BPBP ligands ( $1_{\text{Cu}}$  and  $2_{\text{Cu}}$ ) render an enhanced nuclease activity compared to the parent Cu complexes. Remarkably, Cu metallopeptides  $1_{\text{Cu}}$  and  $2_{\text{Cu}}$  gave a  $\sim 4$ -fold and  $\sim 23$  rate accelerations in comparison with their parent Cu complexes,  $[\text{Cu}(\text{PyTACN})]^{2+}$  and  $[\text{Cu}(\text{BPBP})]^{2+}$ , respectively. Moreover, the apparent DNA binding constants ( $K_{\text{app}}$ ) for  $1_{\text{Cu}}$  and  $2_{\text{Cu}}$  metallopeptides have been found to be 7.1 and 5.9 ( $\times 10^6 \text{ M}^{-1}$ ), respectively, more than 1 order of magnitude higher than those of metal binding conjugates 3 and 4. Although  $1_{\text{Cu}}$  and  $2_{\text{Cu}}$  did not display sequence-specific binding to the DNA, these excellent cleavage abilities are explained by the presence of the cationic tetrapeptide that effectively induces an improved binding affinity to the DNA-minor groove, resulting in groove selectivity on the nuclease activity. Additional mechanistic studies propose that the oxidative cleavage mechanism is based

on the generation of highly reactive oxygen species, causing the DNA damage.

## ■ ASSOCIATED CONTENT

### ■ Supporting Information

The Supporting Information is available free of charge on the ACS Publications website at DOI: [10.1021/acs.inorgchem.5b01680](https://doi.org/10.1021/acs.inorgchem.5b01680).

Additional figures and tables of experimental data (PDF)

## ■ AUTHOR INFORMATION

### Corresponding Author

\*E-mail: [miquel.costas@udg.edu](mailto:miquel.costas@udg.edu)

### Notes

The authors declare no competing financial interest.

## ■ ACKNOWLEDGMENTS

This work was supported by Consolider Ingenio CSD/CSD2010-00065 from MICINN of Spain. We also thank the Catalan DIUE of the Generalitat de Catalunya (2014 SGR 862). X.R. thanks financial support from INNPLANTA project INP-2011-0059-PCT-420000-ACT1. M.C. and X.R. thank ICREA Acadèmia Awards. We also acknowledge the Serveis Tècnics de Recerca of the University of Girona for technical support. J.M. and V.B. thank the Czech Science Foundation (Grants P205/11/0856 and 14-21053S). J.M. and V.B. also acknowledge that their participation in the EU COST Action CM1105 enabled them to exchange regularly the most recent ideas in the field of platinum anticancer drugs with several European colleagues.

## ■ REFERENCES

- (1) Haas, K. L.; Franz, K. J. *Chem. Rev.* **2009**, *109*, 4921–4960.
- (2) Storr, T.; Thompson, K. H.; Orvig, C. *Chem. Soc. Rev.* **2006**, *35*, 534–544.
- (3) Scott, L. E.; Orvig, C. *Chem. Rev.* **2009**, *109*, 4885–4910.
- (4) Lewis, J. C. *ACS Catal.* **2013**, *3*, 2954–2975.
- (5) Ball, Z. T. *Acc. Chem. Res.* **2013**, *46*, 560–570.
- (6) Zeglis, B. M.; Pierre, V. C.; Barton, J. K. *Chem. Commun.* **2007**, 4565–4579.
- (7) Liu, H.-K.; Sadler, P. J. *Acc. Chem. Res.* **2011**, *44*, 349–359.
- (8) Pitié, M.; Pratiel, G. *Chem. Rev.* **2010**, *110*, 1018–1059.
- (9) Mancin, F.; Scrimin, P.; Tecilla, P. *Chem. Commun.* **2012**, *48*, 5545–5559.
- (10) Komor, A. C.; Barton, J. K. *Chem. Commun.* **2013**, *49*, 3617–3630.
- (11) Desbouis, D.; Troitsky, I. P.; Belousoff, M. J.; Spiccia, L.; Graham, B. *Coord. Chem. Rev.* **2012**, *256*, 897–937.
- (12) Jin, Y.; Lewis, M. A.; Gokhale, N. H.; Long, E. C.; Cowan, J. A. *J. Am. Chem. Soc.* **2007**, *129*, 8353–8361.
- (13) Joyner, J. C.; Cowan, J. A. *J. Am. Chem. Soc.* **2011**, *133*, 9912–9922.
- (14) Joyner, J. C.; Reichfield, J.; Cowan, J. A. *J. Am. Chem. Soc.* **2011**, *133*, 15613–15626.
- (15) Puckett, C. A.; Barton, J. K. *J. Am. Chem. Soc.* **2009**, *131*, 8738–8739.
- (16) Heinze, K.; Beckmann, M.; Hempel, K. *Chem. - Eur. J.* **2008**, *14*, 9468–9480.
- (17) Dirscherl, G.; König, B. *Eur. J. Org. Chem.* **2008**, *2008*, 597–634.
- (18) Faller, P.; Hureau, C.; Dorlet, P.; Hellwig, P.; Coppel, Y.; Collin, F.; Alies, B. *Coord. Chem. Rev.* **2012**, *256*, 2381–2396.
- (19) Yu, M.; Price, J. R.; Jensen, P.; Lovitt, C. J.; Shelper, T.; Duffy, S.; Windus, L. C.; Avery, V. M.; Rutledge, P. J.; Todd, M. H. *Inorg. Chem.* **2011**, *50*, 12823–12835.
- (20) Rama, G.; Ardá, A.; Maréchal, J.-D.; Gamba, I.; Ishida, H.; Jiménez-Barbero, J.; Vázquez, M. E.; Vázquez López, M. *Chem. - Eur. J.* **2012**, *18*, 7030–7035.
- (21) Meier, S. M.; Novak, M.; Kandioller, W.; Jakupec, M. a; Arion, V. B.; Metzler-Nolte, N.; Keppler, B. K.; Hartinger, C. G. *Chem. - Eur. J.* **2013**, *19*, 9297–9307.
- (22) Tabassum, S.; Al-Asbahy, W. M.; Afzal, M.; Arjmand, F.; Bagchi, V. *Dalt. Trans.* **2012**, *41*, 4955–4964.
- (23) Blackmore, L.; Moriarty, R.; Dolan, C.; Adamson, K.; Forster, R. J.; Devocelle, M.; Keyes, T. E. *Chem. Commun.* **2013**, *49*, 2658–2660.
- (24) Leonidova, A.; Pierroz, V.; Rubbiani, R.; Lan, Y.; Schmitz, A. G.; Kaech, A.; Sigel, R. K. O.; Ferrari, S.; Gasser, G. *Chem. Sci.* **2014**, *5*, 4044–4056.
- (25) Xing, G.; DeRose, V. J. *Curr. Opin. Chem. Biol.* **2001**, *5*, 196–200.
- (26) Kelso, M. J.; Beyer, L.; Hoang, H. N.; Lakdawala, A. S.; Snyder, J. P.; Oliver, W. V.; Robertson, T. A.; Appleton, T. G.; Fairlie, D. P. *J. Am. Chem. Soc.* **2004**, *126*, 4828–4842.
- (27) Albrecht, M.; Stortz, P. *Chem. Soc. Rev.* **2005**, *34*, 496–506.
- (28) Gamba, I.; Salvadó, I.; Rama, G.; Bertazzon, M.; Sánchez, M. I.; Sánchez-Pedregal, V. M.; Martínez-Costas, J.; Brissos, R. F.; Gamez, P.; Mascareñas, J. L.; Vázquez López, M.; Vázquez, M. E. *Chem. - Eur. J.* **2013**, *19*, 13369–13375.
- (29) Ghesquière, J.; Gauthier, N.; De Winter, J.; Gerbaux, P.; Moucheron, C.; Defrancq, E.; Kirsch-De Mesmaeker, A. *Chem. - Eur. J.* **2012**, *18*, 355–364.
- (30) Li, C.; Zhao, F.; Huang, Y.; Liu, X.; Liu, Y.; Qiao, R.; Zhao, Y. *Bioconjugate Chem.* **2012**, *23*, 1832–1837.
- (31) Suzuki, M. *EMBO J.* **1989**, *8*, 797–804.
- (32) Suzuki, M. *EMBO J.* **1989**, *8*, 4189–4195.
- (33) Huang, H.; Kozekov, I. D.; Kozekova, A.; Rizzo, C. J.; McCullough, A. K.; Lloyd, R. S.; Stone, M. P. *Biochemistry* **2010**, *49*, 6155–6164.
- (34) Cussó, O.; Garcia-Bosch, I.; Ribas, X.; Lloret-Fillol, J.; Costas, M. *J. Am. Chem. Soc.* **2013**, *135*, 14871–14878.
- (35) Company, A.; Prat, I.; Frisch, J. R.; Mas-Ballesté, R.; Güell, M.; Juhász, G.; Ribas, X.; Münck, E.; Luis, J. M.; Que, L., Jr.; Costas, M. *Chem. - Eur. J.* **2011**, *17*, 1622–1634.
- (36) Garcia-Bosch, I.; Gómez, L.; Polo, A.; Ribas, X. *Adv. Synth. Catal.* **2012**, *354*, 65–70.
- (37) Fillol, J. L.; Codolà, Z.; Garcia-Bosch, I.; Gómez, L.; Pla, J. J.; Costas, M. *Nat. Chem.* **2011**, *3*, 807–813.
- (38) Gómez, L.; Garcia-Bosch, I.; Company, A.; Benet-Buchholz, J.; Polo, A.; Sala, X.; Ribas, X.; Costas, M. *Angew. Chem., Int. Ed.* **2009**, *48*, 5720–5723.
- (39) Company, A.; Gómez, L.; Fontrodona, X.; Ribas, X.; Costas, M. *Chem. - Eur. J.* **2008**, *14*, 5727–5731.
- (40) Company, A.; Feng, Y.; Güell, M.; Ribas, X.; Luis, J. M.; Que, L., Jr.; Costas, M. *Chem. - Eur. J.* **2009**, *15*, 3359–3362.
- (41) Codolà, Z.; Garcia-Bosch, I.; Acuña-Parés, F.; Prat, I.; Luis, J. M.; Costas, M.; Lloret-Fillol, J. *Chem. - Eur. J.* **2013**, *19*, 8042–8047.
- (42) Gómez, L.; Canta, M.; Font, D.; Prat, I.; Ribas, X.; Costas, M. *J. Org. Chem.* **2013**, *78*, 1421–1433.
- (43) Jabre, N. D.; Respondek, T.; Ulku, S. a; Korostelova, N.; Kodanko, J. J. *J. Org. Chem.* **2010**, *75*, 650–659.
- (44) Jabre, N. D.; Korostelova, N.; Kodanko, J. J. *J. Org. Chem.* **2011**, *76*, 2273–2276.
- (45) Kaiser, E.; Colescott, R. L.; Bossinger, C. D.; Cook, P. *Anal. Biochem.* **1970**, *34*, 595–598.
- (46) Wyatt, M. D.; Garbiras, B. J.; Haskell, M. A.; Lee, M.; Souhami, R. L.; Hartley, J. A. *Anti-Cancer Drug Des.* **1994**, *9*, 511–525.
- (47) Hernández-Gil, J.; Ferrer, S.; Salvador, E.; Calvo, J.; Garcia-España, E.; Mareque-Rivas, J. C. *Chem. Commun.* **2013**, *49*, 3655–3657.
- (48) Badosa, E.; Ferre, R.; Planas, M.; Feliu, L.; Besalú, E.; Cabrefiga, J.; Bardají, E.; Montesinos, E. *Peptides* **2007**, *28*, 2276–2285.
- (49) Hammoud, M. M.; Mckamie, J. J.; Heeg, M. J.; Kodanko, J. J. *Dalt. Trans.* **2008**, 4843–4845.

- (50) Zhao, M.; Wang, H.-L.; Zhang, L.; Zhao, C.; Ji, L.-N.; Mao, Z.-W. *Chem. Commun.* **2011**, 47, 7344–7346.
- (51) Tjioe, L.; Meininger, A.; Joshi, T.; Spiccia, L.; Graham, B. *Inorg. Chem.* **2011**, 50, 4327–4339.
- (52) Li, Z.-F.; Chen, H.-L.; Zhang, L.-J.; Lu, Z.-L. *Bioorg. Med. Chem. Lett.* **2012**, 22, 2303–2307.
- (53) Tjioe, L.; Joshi, T.; Brugger, J.; Graham, B.; Spiccia, L. *Inorg. Chem.* **2011**, 50, 621–635.
- (54) Skovsen, E.; Snyder, J. W.; Lambert, J. D. C.; Ogilby, P. R. *J. Phys. Chem. B* **2005**, 109, 8570–8573.